GEOLOGICA CARPATHICA, DECEMBER 2021, 72, 6, 482–504 https://doi.org/10.31577/GeolCarp.72.6.3

Petrology and zircon U–Pb dating of granitoid rocks in the Highiş massif (SW Apuseni Mts., Romania): Insights into Permian plutonic–volcanic connections

MÁTÉ SZEMERÉDI[1,2,✉], ANDREA VARGA[2], ISTVÁN DUNKL[3], RÉKA LUKÁCS[1,4], IOAN SEGHEDI[5], ZOLTÁN KOVÁCS[1], BÉLA RAUCSIK[2] and ELEMÉR PÁL-MOLNÁR[1,2]

[1]MTA-ELTE Volcanology Research Group, Pázmány Péter sétány 1/C, H-1117 Budapest, Hungary;
✉szemeredi.mate@gmail.com, reka.harangi@gmail.com, kozraat@gmail.com, palm@geo.u-szeged.hu
[2]Department of Mineralogy, Geochemistry and Petrology, 'Vulcano' Petrology and Geochemistry Research Group, University of Szeged, Egyetem st. 2, H-6722 Szeged, Hungary; raucsikvarga@geo.u-szeged.hu, raucsik@geo.u-szeged.hu
[3]Geoscience Centre, Department of Sedimentology & Environmental Geology, University of Göttingen, Goldschmidtstr. 3, D-37077 Göttingen, Germany; istvan.dunkl@geo.uni-goettingen.de
[4]Institute for Geological and Geochemical Research, Research Centre for Astronomy and Earth Sciences, Eötvös Loránd Research Network (ELKH), Budaörsi út 45, H-1112 Budapest, Hungary
[5]Institute of Geodynamics, Romanian Academy, 19-21 Jean-Luis Calderon St., Bucharest-37, Romania; seghedi@geodin.ro

(Manuscript received March 12, 2021; accepted in revised form September 14, 2021; Associate Editor: Igor Broska)

Abstract: Permian granitoids in the Highiş massif (SW Apuseni Mts., Romania) are anorogenic (A-type), having a peraluminous, subalkaline, alkali-calcic or calc-alkalic, and ferroan character with granodioritic to granitic compositions. Trace elements suggest the crustal origin of the studied samples that derive from a common or similar source associated with post-collisional rifting. Based on trace elements and zircon U–Pb ages (~268–263 Ma), a plutonic–volcanic connection was revealed between the Highiş granitoids and the Mid-Permian (~267–260 Ma) felsic volcanic rocks that are widespread in the Tisza Mega-unit. Felsic plutonic and volcanic rocks (along with mafic–intermediate plutons and lavas in the Apuseni Mts.) represent a Mid-Permian, cogenetic magmatic system. Our results suggest that the study area belongs to the Tisza Mega-unit, in contrast to recent studies considering it as part of the Dacia Mega-unit. Despite the Europe-derived nature of the Tisza Mega-unit, its Permian igneous formations are significantly younger than those of the stable Europe (~300–290 Ma). However, the studied rocks show correlations with some analogous formations in the ALCAPA Mega-unit, including Permian A-type granitoids and felsic volcanic rocks in the Western Carpathians (Gemeric, Veporic, and Silicic Units). On the other hand, many other rocks of similar age in the Western Carpathians and Eastern Alps bear completely different geochemical compositions (S-type character). The latter suggest at least two main types of magma source coevally within the Permo-Triassic post-orogenic setting in the Central European Variscides.

Keywords: Apuseni Mts., Highiş massif, Permian, A-type granitoids, geochemistry, U–Pb, plutonic–volcanic connection.

Introduction

Late Paleozoic times were characterized by intense magmatic activity in the area of the European Variscides. In the Alpine–Carpathian–Pannonian region (i.e. in the Eastern Alps, Western Carpathians, Apuseni Mts., southern Transdanubia, and the basement of the Pannonian Basin) a wide range of Permo–Carboniferous to Lower Triassic felsic plutonic and volcanic rocks occur that are associated with Variscan post-collisional to extensional tectonic events (Fig. 1a; Uher & Broska 1996; Petrík & Kohút 1997; Putiš et al. 2000; Broska & Uher 2001; Pană et al. 2002; Poller et al. 2002; Buda et al. 2004; Vozárová et al. 2009, 2012, 2015, 2016, 2018; Kubiš & Broska 2010; Nicolae et al. 2014; Ondrejka et al. 2018, 2021; Szemerédi et al. 2020a,b; Yuan et al. 2020; Villaseñor et al. 2021). However, palinspastic reconstructions of this Late Paleozoic to Mesozoic realm, where several microplates of distinct origin have broken off the stable European plate along the rift systems on the northern shore of the Paleo-Tethys Ocean (e.g. Stampfli & Kozur 2006), are rather ambiguous and the previous positions of the crustal-scale tectonic blocks of the Central European Variscides, as well as the connections among them are not completely clear. Even local correlations within single mega-units could be problematic due to the complex evolution of the whole Alpine–Carpathian–Pannonian region (Alpine orogeny followed by Neogene extension). In order to establish regional correlations, precise age datings, as well as geochemical studies (including trace elements and isotopes) of the Permo–Triassic rift-related magmatic formations have a crucial role.

Although Western Carpathian granitoids and felsic volcanic rocks were the target of many recent petrological studies (including whole-rock geochemistry and/or zircon/monazite U–Pb geochronology; e.g. Hraško et al. 2002; Poller et al. 2002; Rojkovič & Konečný 2005; Kohút et al. 2009; Vozárová et al. 2009, 2012, 2015, 2016, 2018; Kubiš & Broska 2010;

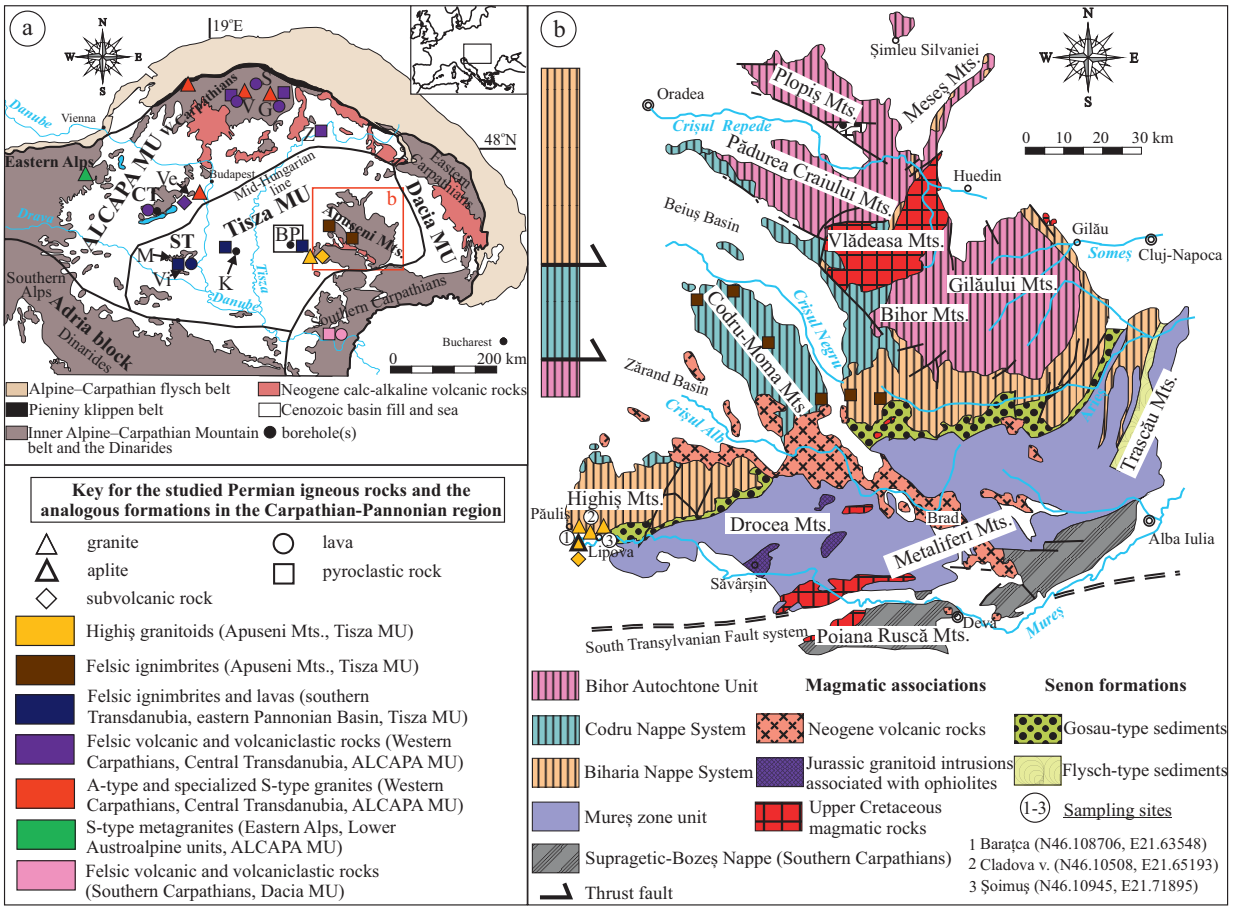

Fig. 1. a — Tectonic sketch of the Carpathian–Pannonian region indicating the subsurface contour of the mega-units, pointing out the occurrences of Permian felsic plutonic (Highiş granitoids) and volcanic rocks in the Tisza Mega-unit, as well as the analogous formations in the ALCAPA and Dacia Mega-units (simplified after Csontos et al. 1992; Csontos & Vörös 2004; Tischler et al. 2008). **b** — Simplified geological map of the Apuseni Mts. (Romania) showing the Alpine tectonic units (see column), the most significant rock assemblages, and the localities of the studied granitoid samples with GPS coordinates (modified after Bleahu 1976; Ianovici et al. 1976; Săndulescu 1984; Balintoni et al. 2009; Ionescu & Hoeck 2010). Abbreviations: BP=Battonya–Pusztaföldvár Basement Ridge, CT=Central Transdanubia, G=Gemeric Unit, K=Kelebia area, M=Mecsek Mts., MU=mega-unit, S=Silicic Unit, ST=southern Transdanubia, V=Veporic Unit, Ve=Velence Mts., Vi=Villány Mts., Z=Zemplinic Unit.

Broska & Petrík 2015; Ondrejka et al. 2018, 2021; Broska & Svojtka 2020; Villaseñor et al. 2021), much less research was carried out on the similar formations of the Tisza and the Dacia Mega-units (Fig. 1a). Nevertheless, ongoing studies could suggest a significant correlation among the Late Paleozoic magmatic formations of the Tisza Mega-unit, corresponding to the areas of southern Transdanubia and the eastern Pannonian Basin (Hungary), with the similar magmatic rocks of the Apuseni Mts. (Romania; Szemerédi et al. 2020a,b; Fig. 1a,b). Despite their occurrence in various locations and Alpine tectonic units of the Tisza Mega-unit, petrography, whole-rock geochemistry, and zircon U–Pb geochronology of the Permian silicic volcanic rocks revealed a Mid-Permian (~267–260 Ma) voluminous volcanism, the products of which occur from the Western Mecsek Mts. (southern Transdanubia; Fig. 1a) to the Codru-Moma and Bihor Mts. (Apuseni Mts.; Fig. 1b). Moreover, some kind of plutonic–volcanic connections could be assumed between the Permian A-type (anorogenic; Bonin & Tatu 2016) granitoids of the Highiş massif (SW Apuseni Mts.; for those, henceforth, the term 'Highiş granitoids' is used in this study; Fig. 1b) and the aforementioned felsic volcanic rocks (ignimbrites and subordinate lavas) of the Tisza Mega-unit (Nicolae et al. 2014; Szemerédi et al. 2020a; Fig. 1a). Although the Highiş granitoids were studied in the last decades from several, distinct points of view (e.g. Pană et al. 2002; Pál-Molnár et al. 2008; Bonin & Tatu 2016), the sporadic nature of the bulk geochemical datasets, as well as a singular radiometric age datum (measured on the Jernova porphyritic microgranite that represents a subordinate lithology of the granitoid rocks; Pană et al. 2002) made it impossible to gain unequivocal implications about their genetic connections.

Thereby, the major aims of this study are (1) to complete the available information about the Highiş granitoids with additional results in detailed petrography, whole-rock geochemistry (including major and trace elements), and zircon U–Pb geochronology and (2) to explore their plutonic–volcanic connection with the Permian felsic volcanic rocks in

the Tisza Mega-unit (Apuseni Mts., basement of the eastern Pannonian Basin, southern Transdanubia) by reliable geochemical and geochronological evidence. Moreover, (3) the zircon U–Pb ages, as well as the whole-rock geochemical results are compared to those of the Permian felsic magmatic rocks in the Central European Variscides (paying special attention to the Western Carpathians, in which case some linkage was also assumed previously; Varga & Raucsik 2014; Szemerédi et al. 2020a; Fig. 1a) in order to gain new information about regional aspects. By the latter, our goal is not only to determine the geotectonic environment and the magma generation of the studied Highiş granitoids, but also to locate the magmatism in time among the similar Late Paleozoic post-orogenic events in the Paleo-Tethyan realm.

Geological background

The Apuseni Mts. (Fig. 1b) are located between the Pannonian and the Transylvanian Basins showing a present-day structure that reflects the result of complex Alpine tectonic events (Balla 1984; Kovács 1992; Csontos et al. 1992). Four distinct tectonic units are separated in the area of the Apuseni Mts. from bottom to top: (1) Bihor Autochtone Unit, (2) Codru Nappe System, (3) Biharia Nappe System, and (4) Mureş zone unit (Bleahu et al. 1981; Balintoni 1997; Balintoni et al. 2009; Fig. 1b). The basement of the first three abovementioned units comprises Precambrian to Late Paleozoic polymetamorphic series, including the products of three large igneous episodes (Late Cambrian, Middle to Late Devonian, and Early Permian in age; Pană et al. 2002). Basement formations are usually covered by upper Paleozoic and Mesozoic sedimentary and/or volcanic rocks (Nicolae et al. 2014). While the Bihor Autochthone Unit and Codru Nappe System in the Apuseni Mts. unequivocally represent the Tisza Mega-unit, the area of the Biharia Nappe System that includes the Highiş granitoids is still a matter of debate. According to some previous studies (e.g. Csontos & Vörös 2004), the Biharia Nappe System (as its highest Alpine tectonic unit) belongs to the Tisza Mega-unit. On the other hand, other recent tectonostratigraphic studies suggest that the Biharia Nappe System belongs to the Dacia Mega-unit (e.g. Schmid et al. 2008, 2020; Gallhofer et al. 2016).

The Highiş igneous complex consists of mafic–intermediate (gabbro, diorite, and granodiorite, respectively) and anorogenic, felsic A-type (alkali-feldspar granite, including albite granite) rocks (Pană et al. 2002; Bonin & Tatu 2016). Based on the zircon U–Pb dating of the Jernova porphyritic microgranite (264.2±2.3 Ma) and the Cladova diorite (266.7±3.8 Ma), plutonism was a relatively short, Mid-Permian event (Pană et al. 2002). According to the previous geochemical results, including whole-rock geochemistry and mineral chemistry, the Highiş granitoids are felsic-peraluminous alkali granites, with alkali-calcic character formed in a post-collisional (post-orogenic) tectonic setting (Pál-Molnár et al. 2008) that refers to the possible rift-related origin of these rocks.

On the other hand, the Permian volcanic rocks are mostly felsic ignimbrites and mafic-intermediate lavas, representing a bimodal suite. They are exposed in the central–western part of the Apuseni Mts. (Codru-Moma and Bihor Mts.), being relatively abundant in the Codru Nappe System, less prevalent in the Biharia Nappe System and sporadic in the Bihor Autochthone Unit (Nicolae et al. 2014; Fig. 1b). The whole-rock geochemical composition of these felsic volcanic rocks (Nicolae et al. 2014) implies a strong correlation with the similar formations in the basement of the eastern Pannonian Basin and southern Transdanubia (267–260 Ma, pyroclastic rocks and lavas; Szemerédi et al. 2020a,b). Moreover, feasible plutonic–volcanic connections could be assumed between the Highiş granitoids and the Permian felsic volcanic rocks of the Tisza Mega-unit, taking into consideration their convincingly similar geochemical characteristics and the available geochronological results (Pană et al. 2002; Szemerédi et al. 2020a). Besides the aforementioned suggestions, the necessity of further geochemical (trace elements) and geochronological (zircon U–Pb datings) investigations of the Highiş granitoids has been emphasized as well.

When it comes to the observation of Paleozoic magmatic formations, we should take into account that such rocks might be affected by various post-magmatic alterations. The study area (see sampling details in the next chapter; Fig. 1b) is cut across by a Variscan greenschist facies shear zone, the so-called Highiş-Biharia Shear Zone (Pană et al. 2002; Ciobanu et al. 2006) that reactivated during the Alpine tectonic events, as well. Although plutonic bodies were partially preserved as low strain pods during Alpine shearing, some parts were significantly overprinted (Pană & Balintoni 2000; Pană et al. 2002). Moreover, whole-rock and mineral chemical data revealed various degrees of metasomatic and hydrothermal alterations of the Permian magmatic formations (Ciobanu et al. 2006; Nicolae et al. 2014; Bonin & Tatu 2016; Szemerédi et al. 2020a). Hence, their petrogenetic implications are basically based on the immobile trace elements.

Sampling and analytical methods

Samples were collected in the Highiş Mts. (SW Apuseni Mts.) from three distinct abandoned quarries (Fig. 1b; Table 1). In the Baraţca quarry, the dominant medium-grained granites are crosscut by aplites, furthermore subordinate porphyritic microgranites also occur in this locality. All of these three lithologies were collected and studied from the quarry. Nearby Baraţca, another outcrop of medium-grained granites was sampled at the intersection of the Cladova creek and the E68 main road (Cladova valley quarry). The third sampling site (Şoimuş quarry) is situated at the western side of Şoimuş (castle) hill. The latter is generally made up of granitoid rocks affected by Alpine shearing; however, on the macroscopic scale, undeformed medium-grained granite samples were collected in this quarry.

Table 1: Sampling details, mineralogical composition (point counting by JMicroVision software; Roduit 2019), and petrographic classification (according to the Streckeisen diagram) of representative rock samples (granites, microgranites, and aplites) of the Permian Highiş granitoids, Apuseni Mts. Names of the three samples that were targeted by zircon U–Pb datings are highlighted by grey. Abbreviations: bt=biotite, mc=microcline, ms=muscovite, mx=matrix, or=orthoclase, pl=plagioclase, qz=quartz.

Sample	Quarry, GPS coordinates	Rock type	Or	Qz	Mc	Pl	Bt	Ms	Mx	Classification
HGBC1	Baraţca N46.10875 E21.63563	granite	37.4	46.2	5.0	7.7	3.6	0	0	syenogranite
HGBC2			47.2	39.4	5.2	4.8	3.4	0	0	alkali-feldspar granite
HGBC3			44.6	41.4	4.6	6.4	2.6	0.4	0	syenogranite
HGCL1	Cladova valley N46.10508 E21.65193	granite	40.4	39.4	8.8	8.2	2.6	0.4	0	syenogranite
HGCL2			38.8	43.5	7.5	5.0	4.3	0.8	0	syenogranite
HGSO1	Şoimuş N46.10945 E21.71895	granite	46.2	34.2	8.2	5.8	5.6	0	0	syenogranite
HGSO2			42.0	37.0	7.4	4.8	8.4	0.4	0	alkali-feldspar granite
HGBM1	Baraţca N46.10858, E21.63432	micro-granite	6.4	3.0	2.6	0.8	0.4	0.2	86.6	alkali-feldspar granite
HGBM2			4.6	4.6	2.6	0.8	1.0	0	86.4	alkali-feldspar granite
HGBAP1	Baraţca N46.10876, E21.63401	aplite	37.8	44.0	10.4	6.8	1.0	0	0	syenogranite
HGBAP2			37.2	43.0	12.2	7.2	0.4	0	0	syenogranite
HGBAP3			39.2	42.0	11.4	6.0	1.4	0	0	syenogranite

Petrographic studies, including mineralogical and textural observations, were conducted on both hand specimens (35) and thin sections (18). On thin section scale, modal compositions of rock-forming minerals were measured by point counting. A total of 12 unaltered or barely altered, representative samples, including medium-grained granites, microgranites, and aplites were investigated (at least 500 points were counted per thin section; Table 1), using the JMicroVision software (Roduit 2019). Petrographic descriptions were supplemented by scanning electron microscope (SEM) analyses of accessory components, using an AMRAY 1830 SEM at the Department of Petrology and Geochemistry, Eötvös Loránd University, Budapest. At certain points, petrography was supported by previous mineral chemical data (microprobe analyses of feldspar, biotite, and muscovite published by Pál-Molnár et al. 2008).

The same samples were selected for whole-rock geochemistry (Table 2), as well. Rock specimens were powdered and analyzed at the Bureau Veritas Mineral Laboratories (Acme-Labs, Vancouver, Canada) by ICP-ES (major elements) and ICP-MS (trace elements). Laboratory conditions were the same as those for the previously studied Permian felsic volcanic rocks in the Tisza Mega-unit (see details in Szemerédi et al. 2020a), providing a proper comparison of the results.

Zircon crystals of 63–250 µm size were separated from 3 distinct medium-grained granite samples (Baraţca, Cladova valley, and Şoimuş quarries; Table 1) by standard heavy mineral separation method (crushing, sieving, heavy liquid separation, magnetic separation, and hand-picking). The grains were fixed on a double-side adhesive tape then embedded in epoxy mounts of 25 mm diameter. The mounts were lapped by 2500 mesh SiC paper then polished by 6, 3, and 1 micron diamond suspensions. Cathodoluminescence mapping of the zircon crystals occurred at the Department of Petrology and Geochemistry, Eötvös Loránd University, Budapest, using an AMRAY 1830 SEM equipped with a GATAN MiniCL detector.

In-situ U–Pb age determinations (Supplementary Table S1) were performed at the GÖochron Laboratories of Georg-August University, Göttingen by laser-ablation single-collector sector-field inductively coupled plasma mass spectrometry (LA–SF–ICP–MS). A Thermo Scientific Element 2 mass spectrometer was used, coupled to a Resonetics Excimer laser ablation system. All age data presented here were obtained by single spot analyses mostly in the mantles of the zircon crystals, in order to avoid antecrystic cores, with laser beam diameters of 33 or 23 µm, a repetition rate of 5 Hz, an energy density of ca. 2 J cm^{-2}, and a crater depth of approximately 10 µm.

Data reduction was based on the processing of 46 time slices (corresponding to ca. 13 s) starting ca. 3 s after the beginning of the signal. When the ablation hit zones or inclusions with variable isotope ratios, the integration interval was resized or the analysis was rejected. Individual time slices were tested for possible outliers by an iterative Grubbs test (at P=5 % level). This test filtered out only the extremely biased time slices and in this way usually less than 2 % of the time slices were discarded. Drift and fractionation corrections, as well as data reductions were done by an in-house software (UranOS; Dunkl et al. 2008). Age calculation and quality control were based on the drift and fractionation correction by standard-sample bracketing using GJ-1 as primary zircon standard reference material (Jackson et al. 2004). For further control, the Plešovice and the 91500 zircons were analyzed as secondary standard reference materials (Wiedenbeck et al. 1995; Sláma et al. 2008). The age results of the aforementioned reference materials were consistently within 2 SE of the published ID-TIMS values.

Concordia plots and age spectra were constructed and age calculations were done by the Isoplot/Ex 3.0 (Ludwig 2012) and the IsoplotR (Vermeesch 2018) softwares. Measurements were considered discordant if the difference between the $^{207}Pb/^{235}U$ and $^{206}Pb/^{238}U$ dates was larger than 10 % (Supplementary Table S1). Discordant results are typically

Table 2: Major and trace element data of the studied Permian granitoid rocks in the Apuseni Mts. Geochemical parameters of the samples such as ASI (aluminium saturation index), MALI (modified alkali-lime index), Fe/Fe+Mg (Fe-number), A/NK, and A/CNK were calculated after Shand (1943), Frost et al. (2001), and Frost & Frost (2008). Zircon saturation temperatures were calculated by the method introduced by Boehnke et al. (2013). $Eu/Eu^* = [Eu_N/(Sm_N \times Gd_N)^{1/2}]$; $Ce/Ce^* = [Ce_N/(La_N \times Pr_N)^{1/2}]$; N = chondrite-normalized values, chondrite data from Barrat et al. (2012). Major element concentrations are given in wt. %, while trace elements in ppm. Ni concentrations were measured but not detected (<20 ppm).

Sample	HGBC1	HGBC2	HGBC3	HGCL1	HGCL2	HGSO1	HGSO2	HGBM1	HGBM2	HGBAP1	HGBAP2	HGBAP3
SiO_2	74.76	75.69	74.85	75.91	75.11	74.16	73.42	76.69	76.52	76.50	76.80	76.01
TiO_2	0.18	0.18	0.19	0.18	0.20	0.25	0.26	0.07	0.07	0.17	0.15	0.12
Al_2O_3	12.70	13.25	12.67	12.54	12.76	13.12	13.30	12.38	12.30	13.73	13.74	14.09
Fe_2O_3t	2.18	1.67	2.32	1.89	1.95	2.24	2.32	1.39	1.64	0.69	0.60	0.79
MnO	0.04	0.01	0.01	0.03	0.02	0.02	0.03	0.02	0.02	0.01	0.00	0.00
MgO	0.18	0.90	0.04	0.19	0.10	0.19	0.19	0.04	0.05	0.03	0.02	0.24
CaO	0.54	0.13	0.09	0.14	0.42	0.46	0.41	0.13	0.15	0.52	0.12	0.11
Na_2O	3.56	5.16	3.72	4.12	3.80	4.39	3.69	3.71	3.75	7.89	8.03	7.85
K_2O	4.71	1.86	5.48	4.19	4.97	3.88	4.98	5.01	4.74	0.17	0.15	0.30
P_2O_5	0.05	0.05	0.07	0.07	0.06	0.08	0.06	0.03	0.03	0.06	0.07	0.05
LOI	1.00	1.00	0.40	0.60	0.50	1.10	1.10	0.40	0.60	0.20	0.20	0.30
sum	99.92	99.92	99.84	99.86	99.92	99.91	99.76	99.87	99.93	99.96	99.88	99.86
Ba	402	202	451	331	415	423	474	86	102	18	14	19
Sc	4	4	4	5	3	5	6	4	4	1	<1	2
Rb	189.5	112.1	159.8	170.3	142.8	127.2	164.1	246.7	240.9	4.9	4.4	24.6
Cs	5.4	3.5	1.0	9.2	2.1	3.2	4.5	2.9	2.9	0.1	0.2	1.5
Y	49.8	54.3	43.0	21.9	27.7	33.8	36.5	44.4	53.6	37.1	51.4	21.9
La	36.3	30.3	42.3	21.6	29.9	41.3	40.9	18.3	23.0	11.6	24.8	14.7
Ce	73.2	28.8	96.9	44.7	66.3	83.3	71.5	38.6	46.3	14.6	34.9	32.5
Pr	8.87	7.89	10.79	5.19	7.59	9.22	10.06	4.28	6.00	3.01	6.98	3.46
Nd	33.6	31.2	39.6	18.8	28.7	34.1	37.3	15.3	22.1	13.4	28.7	14.8
Sm	7.55	7.93	8.17	3.89	6.25	6.77	7.85	3.73	5.80	3.76	8.04	3.28
Eu	0.61	0.56	0.62	0.28	0.44	0.53	0.69	0.12	0.13	0.29	0.60	0.23
Gd	7.97	8.76	7.39	3.58	5.24	6.34	7.09	4.18	6.65	4.76	9.02	3.50
Tb	1.37	1.47	1.27	0.65	0.90	1.00	1.15	0.90	1.32	0.88	1.57	0.59
Dy	8.14	8.70	7.56	4.24	5.43	5.92	6.58	6.27	8.90	5.55	8.97	3.52
Ho	1.80	1.89	1.63	0.98	1.10	1.24	1.37	1.50	1.94	1.27	1.93	0.80
Er	5.27	5.67	4.96	3.36	3.46	3.73	4.16	5.49	6.31	4.05	5.25	2.59
Yb	5.16	5.50	5.17	4.27	3.84	3.61	4.01	8.16	7.82	4.00	4.46	2.80
Lu	0.77	0.86	0.73	0.65	0.61	0.56	0.61	1.29	1.25	0.62	0.65	0.44
Th	17.9	18.6	16.2	16.3	17.0	18.9	16.8	19.4	33.0	16.6	16.8	12.5
U	5.4	5.6	3.8	3.4	2.9	3.9	3.7	6.2	6.1	5.1	4.2	2.9
V	8	<8	12	<8	90	14	18	<8	<8	<8	<8	<8
Co	1.9	1.3	2.2	3.7	2.0	2.3	1.6	0.5	1.3	0.6	0.5	2.0
Zr	174.9	185.3	167.3	174.7	180.3	237.6	240.8	153.7	140.2	199.7	180.2	185.5
Nb	11.5	11.5	9.1	9.2	10.1	9.4	9.1	18.5	17.7	15.8	15.2	11.5
Hf	6.4	6.8	5.9	6.2	6.4	7.3	7.5	8.4	7.9	6.8	6.4	6.0
Ta	1.2	1.2	0.8	1.0	0.9	1.1	1.0	1.3	1.4	1.2	1.0	0.8
Ga	19.3	20.0	13.3	17.6	19.5	20.1	18.7	20.7	21.1	18.6	17.4	19.3
Be	4	6	3	3	5	3	2	5	6	5	2	6
Sn	10	42	6	5	5	4	5	13	13	26	23	30
Sr	31.5	10.0	22.2	16.7	27.1	31.1	38.9	12.7	14.4	14.9	8.7	8.4
W	2.8	4.1	1.5	1.2	1.2	1.5	1.3	1.6	4.7	1.1	1.0	0.9
Tm	0.78	0.83	0.76	0.58	0.53	0.55	0.64	1.07	1.06	0.61	0.75	0.41
$(La/Yb)_N$	5.03	3.94	5.85	3.62	5.57	8.18	7.29	1.60	2.10	2.07	3.98	3.75
$(La/Sm)_N$	3.13	2.49	3.37	3.62	3.11	3.97	3.39	3.19	2.58	2.01	2.01	2.92
$(Gd/Yb)_N$	1.26	1.30	1.17	0.68	1.11	1.43	1.44	0.42	0.69	0.97	1.65	1.02
Eu/Eu*	0.24	0.20	0.24	0.23	0.23	0.25	0.28	0.09	0.06	0.21	0.21	0.21
Ce/Ce*	0.99	0.45	1.11	1.03	1.07	1.04	0.86	1.06	0.96	0.60	0.65	1.11
∑REE	191.39	140.36	227.85	112.77	160.29	198.17	193.91	109.19	138.58	68.40	136.62	83.62
ASI	1.08	1.24	1.04	1.09	1.04	1.08	1.10	1.06	1.07	0.98	1.02	1.05
MALI	7.81 C-A	6.97 C-A	9.16 A-C	8.23 A-C	8.40 A-C	7.90 A-C	8.37 A-C	8.64 A-C	8.40 A-C	7.56 C-A	8.09 C-A	8.08 C-A
Fe/Fe+Mg	0.92 F	0.63 M	0.98 F	0.90 F	0.95 F	0.91 F	0.92 F	0.97 F	0.97 F	0.95 F	0.96 F	0.75 M
A/NK	1.16	1.26	1.05	1.11	1.10	1.15	1.16	1.07	1.09	1.04	1.03	1.06
A/CNK	1.11	1.25	1.04	1.10	1.06	1.11	1.12	1.06	1.08	1.01	1.02	1.06
Zircon T_{sat} (°C)	757	786	748	762	755	789	793	745	737	753	750	758

caused by common Pb contamination (either from inclusions or from cracks) or by recent Pb-loss by the leaching of the zircon crystals accumulated relatively high alpha damage densities.

The total external error is composed of the uncertainty from (1) the corrections being applied (drifting along the measurement sequence and the down hole fractionation correction), (2) uncertainty of the decay constants, and (3) the uncertainty of the $^{206}Pb/^{238}U$ ratio of the GJ-1 primary standard reference material. Crystallization ages were calculated with 95 % confidence and total uncertainties (quadratically propagated external errors) are given as suggested in Horstwood et al. (2016).

Results and interpretation of data

Petrography

Medium-grained, equigranular, subhedral granular syenogranites (Baraţca, Cladova valley, and Şoimuş quarries)

Medium-grained granites, corresponding to the most common lithology of the Highiş granitoids in the study area, consist of orthoclase (40–47 vol. %), quartz (34–46 vol. %), microcline (5–9 vol. %), plagioclase (5–8 vol. %), and biotite (3–8 vol. %) as rock-forming minerals that have rather similar grain size distribution (average size: 1–3 mm, maximum size: 5–6 mm, except for microcline and biotite that are not coarser than 2.5 and 1 mm, respectively; Fig. 2a–d). Biotite crystals appear in a much smaller size (0.2–0.8 mm) than the other components, forming 1–2 mm sized crystal clots (Fig. 2c). Additionally, muscovite (<1 vol. %; Fig. 2d) occurs in smaller amounts as a secondary mineral (see description below). Zircon and apatite crystals are excessively frequent, in minor amounts monazite, thorite, ilmenite, and Fe-oxides were also observed. These accessory components are most commonly associated with the clots of biotite.

Orthoclase crystals (Fig. 2a–d) are subhedral, mildly sericitized and occasionally show Carlsbad twins (Fig. 2a). Their average size is 1.5–3 mm, while the coarsest grains might reach 6 mm. In some of them, relatively small (0.2–0.3 mm), euhedral to subhedral plagioclase inclusions (Fig. 2b) occur.

Quartz grains (Fig. 2a–d) are generally subhedral to anhedral, resorbed, often fragmented and/or deformed monocrysts (Fig. 2a,c); however, polycrystalline varieties (i.e. subgrains; Fig. 2d) also occur. The average size of the crystals is 1–3 mm, while the coarsest quartz grains might reach 5 mm.

Microcline crystals (Fig. 2a,b,d) are subhedral to anhedral and show tartan twinning. Their average size is 0.5–1.5 mm, while the maximum size is 2.5 mm.

Plagioclase feldspars (Fig. 2b–d) are euhedral to subhedral, variably sericitized or carbonatized and show polysynthetic twins. Their average size is 1–3 mm, while their maximum size is 5 mm. In some samples plagioclases occur in crystal clots, as well. According to our previous mineral chemical study (Pál-Molnár et al. 2008), all of the plagioclase grains have an albite-rich feldspar composition ($Ab_{94–100}$).

Biotite crystals (Fig. 2b–d) are generally subhedral and affected by various degrees of alterations (replaced by secondary Fe-oxides or chlorite). Nevertheless, idiochromatic, relatively fresh crystals (Fe-rich varieties: magnesian-siderophyllites or ferroan-phlogopites, based on previous microprobe analyses; Pál-Molnár et al. 2008) are common, too. Their average size ranges between 0.2 and 0.8 mm, while the largest crystals might reach 1 mm. Şoimuş quarry (Fig. 2d) differs from the other localities by its granites containing significantly more biotite crystals (6–8 vol. % in contrast to the average 3–4 vol. %; Table 1).

Euhedral to subhedral muscovite crystals (in 0.2–0.4 mm size) are rather subordinate and associated with the clots of biotite (Fig. 2d), as well as the areas of intense sericitization. All the latter suggest their secondary origin, being in accordance with their chemical composition (Pál-Molnár et al. 2008).

According to their mineralogical composition (Table 1), the observed rocks are syenogranites and subordinate alkali-feldspar granites.

Porphyritic microholocrystalline subvolcanic rocks (microgranites; Baraţca quarry)

Porphyritic microgranite (Fig. 2e,f) occurs only in the Baraţca quarry of the studied areas where this rock type represents a subordinate amount of the whole material. The samples consist of 13–14 vol. % medium-grained porphyres (orthoclase, quartz, microcline, plagioclase, and biotite; Table 1) in a microholocrystalline matrix (86–87 vol. %) of quartz, K-feldspar, and plagioclase (50–200 μm sized crystals). Phenocrystals (average size: 1–1.5 mm, maximum size: 3 mm) and accessory components show quite similar characteristics to those of the medium-grained, equigranular syenogranites; however, feldspar (8–10 vol. %) and quartz (3–5 vol. %) crystals are bordered by irregular, fringy margins instead of clearly-visible, continuous edges (Fig. 2e,f). Moreover, polycrystalline quartz grains do not occur in these samples and the amount of sericitized and/or carbonatized plagioclase is subordinate (<1 vol. %) compared to other lithologies. According to the mineralogical composition, such subvolcanic rocks (microgranites) are basically alkali-feldspar granites (Table 1).

Medium-grained, equigranular, subhedral granular aplites (Baraţca quarry)

Aplites (Fig. 2g,h) are macroscopically easily distinguishable from the medium-grained syenogranites based on their greyish white colour. They occur in the Baraţca quarry showing subvertical arrangement within the main granitic part. Their textural features are quite similar to those of the syenogranites (medium-grained, equigranular, subhedral granular texture); however, these samples are relatively unaltered or completely fresh. Their major mineral assemblage consists of quartz

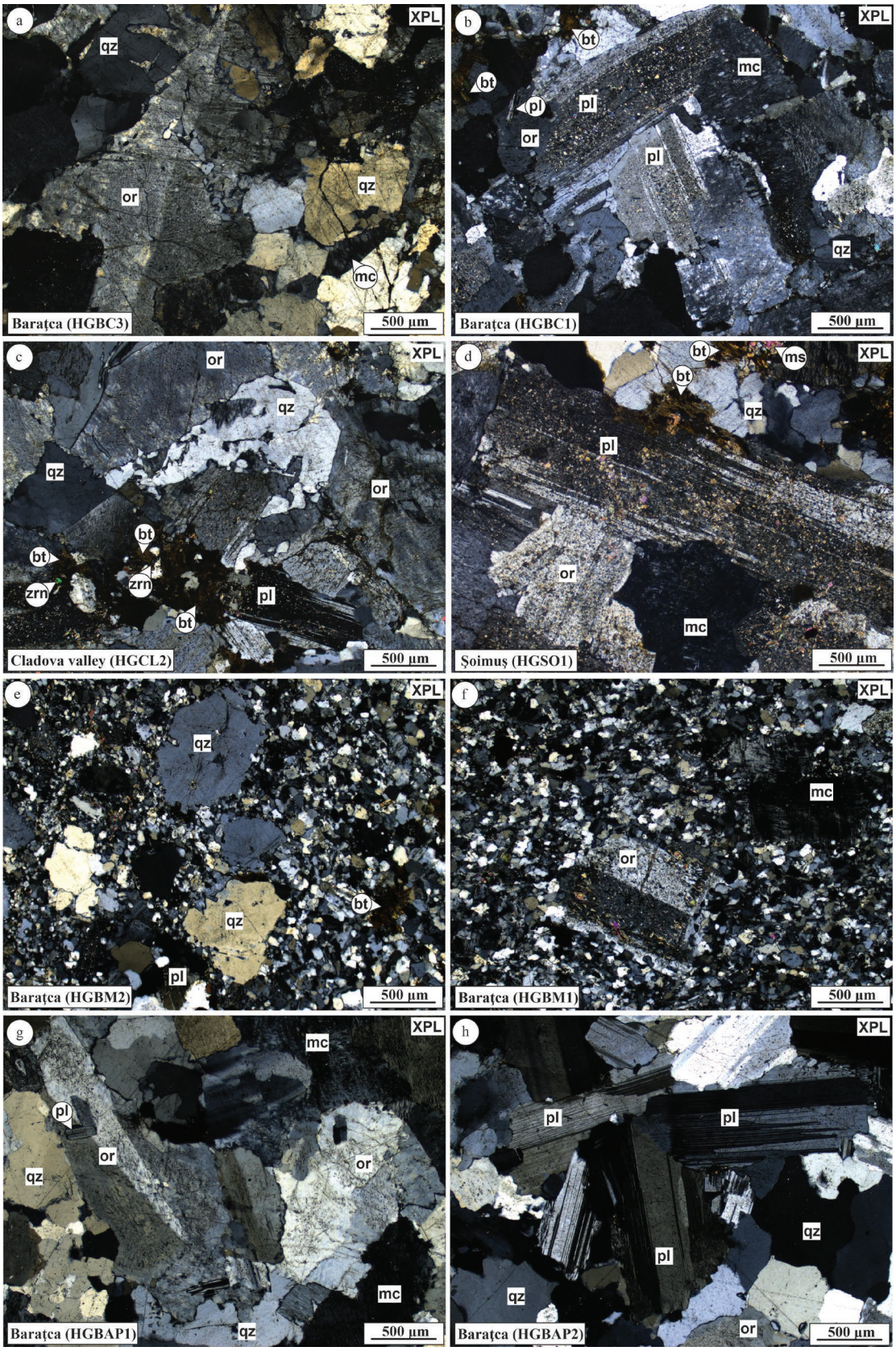

Fig. 2. Photomicrographs of the Highiş granitoids, Apuseni Mts. **a–d** — Medium-grained, equigranular, subhedral granular syenogranites from the Barațca, the Cladova valley, and the Şoimuş localities; **e–f** — Porphyritic microholocrystalline subvolcanic rocks (microgranites) from the Barațca quarry; **g–h** — Medium-grained, equigranular, subhedral granular aplites from the Barațca quarry. Abbreviations: bt=biotite, mc=microcline, ms=muscovite, or=orthoclase, pl=plagioclase, qz=quartz, zrn=zircon, XPL=crossed polars.

(42–44 vol. %; Fig. 2g,h), orthoclase (37–39 vol. %; Fig. 2g,h), microcline (10–12 vol. %; Fig. 2g), plagioclase (6–7 vol. %; Fig. 2h), and subordinate biotite (0–1.5 vol. %). Their high microcline and low biotite contents support the aplitic origin and distinguish these rocks from the common syenogranites of the area. The main petrographic and geochemical (Pál-Molnár et al. 2008) characteristics of rock-forming minerals, as well as the occurrence of accessory components do not differ significantly from those of the latter; however, the lack of alterations should be emphasized. Grain sizes are slightly finer (average: 1–2 mm, maximum: 3 mm, except for the 0.2–0.6 mm sized biotite crystals) than those of the medium-grained granites. According to their mineralogical composition, aplites are classified as syenogranites, as well.

Major and trace element geochemistry

Major and trace elements were analyzed for representative samples of all of the studied lithologies (granite, microgranite, and aplite) and localities of the Highiş granitoids (Table 2). For geochemical comparison, compositions of the Permian felsic volcanic rocks (ignimbrites and subordinate lavas) from southern Transdanubia and the basement of the eastern Pannonian Basin (Hungary, Fig. 1a; Szemerédi et al. 2020a), as well as felsic ignimbrites from the Apuseni Mts. (Codru-Moma and Bihor Mts., Fig. 1b; Nicolae et al. 2014) were plotted in some of the geochemical diagrams, too. Moreover, published bulk geochemical data of the Permian granitoid and felsic volcanic rocks of the broader area (Alpine–Carpathian–Pannonian region, including the Eastern Alps, Western Carpathians, and Central Transdanubia; Fig. 1a) were also plotted in the diagrams for comparison. Potential plutonic–volcanic connections, as well as the regional correlations of the studied granitoid rocks are discussed in detail in the following chapter.

In the total alkali-silica (TAS) diagram (Fig. 3a), all of the studied samples fall into the rhyolite (granite) field with 74.4–77.1 wt. % SiO_2 and relatively high (7.1–9.3 wt. %) alkali contents. As Paleozoic magmatic rocks might be affected by various post-magmatic alterations (e.g. Nicolae et al. 2014; Bonin & Tatu 2016; Szemerédi et al. 2020a; Villaseñor et al. 2021), rock classifications were also carried out using the Zr/TiO_2 vs. Nb/Y diagram (Fig. 3b). Such elemental ratios are less sensitive for secondary processes. In this diagram, medium-grained granites plot in the rhyodacite/dacite (granodiorite) field and only porphyritic microgranites and aplites fall into the rhyolite (granite) field. Both the TAS and the Zr/TiO_2 vs. Nb/Y diagrams refer to the subalkaline character of the Highiş granitoids (Fig. 3a,b).

In the A/NK vs. A/CNK diagram (Shand 1943), all of the granitoid rocks proved to be slightly peraluminous (A/NK= 1.0–1.2, A/CNK=1.0–1.1; Table 2). Only one granite sample (HGBC2) showed mildly higher values (A/NK=1.3, A/CNK=1.3) that might be in accordance with the moderate post-magmatic alterations observed in the rock. According to the aluminium saturation index (ASI; Table 2; Frost & Frost 2008), that ranges between 1.0 and 1.1, the studied granites are peraluminous, as well. Further geochemical characterizations of Frost et al. (2001) and Frost & Frost (2008) suggested that the Highiş granitoids have alkali-calcic or calc-alkalic (MALI=7.6–9.2; Table 2; Fig. 3c) and dominantly ferroan (Fe/Fe+Mg=0.6–1.0; Table 2; Fig. 3d) character.

For the classification of granitoid rocks, diagrams were introduced by Whalen et al. (1987) that could discriminate anorogenic (A-type) granites from other (S, I, and M) types. In most of these diagrams (Fig. 3e–g), regardless of the contents of major or trace elements, the Highiş granitoids plot in the A-type field. Their A-type character involves, besides the previously mentioned high SiO_2 and alkali contents, high Fe/Mg ratios (ferroan character), low Ca and Sr contents, and relatively large high field strength elements (HFSEs) concentrations. For the further subdivision of anorogenic granites, Eby (1992) introduced a set of discrimination diagrams (e.g. Nb–Y–Ce and Nb–Ga–Y diagrams), according to which all of the studied samples plot in the A2-type field, corresponding to the magmas derived from continental crust or underplated crust (Fig. 3h).

Further geotectonic implications were gained by the discrimination diagrams of Pearce et al. (1984) introduced for granitoid rocks (Fig. 4a–d). In these diagrams (Y–Nb, Yb–Ta, Yb+Ta–Rb, and Y+Nb–Rb) the Highiş granitoids fall into the border of the volcanic arc granite (VAG) and the within plate granite (WPG) fields, suggesting the formation of the rocks in a post-collisional to extensional (post-orogenic) environment.

In general, the studied samples are strongly enriched in rare-earth elements (REEs) and show fractionated REE patterns, expressed by the La_N/Yb_N ratio (1.6–8.2), with respect to chondrite composition (Table 2; Fig. 5a). Total REE (ΣREE) values, however, lie in a relatively broad range from 68 ppm to 228 ppm (samples HGBAP1 and HGBC3, respectively; Table 2). In the chondrite-normalized REE diagram (Fig. 5a), granites and microgranites display enriched light (La_N/Sm_N= 2.6–4.0) REE patterns; however, in contrast to the near-flat heavy REE patterns of the granites (Gd_N/Yb_N=0.7–1.4), slightly higher concentrations of Er to Lu were observed in the case of microgranites (Gd_N/Yb_N = 0.4–0.7). On the other hand, aplites differ from the lithologies mentioned above, showing a slightly lower enrichment in light REEs (La_N/Sm_N = 2.0–2.9) and slightly higher enrichment in heavy REEs (Gd_N/Yb_N=1.0–1.7). All of the studied samples are characterized by variously deep negative Eu anomaly (Eu/Eu*= 0.1–0.3; Table 2; Fig. 5a) indicating the feldspar fractionation. It is noteworthy that three samples (HGBC2, HGBAP1, HGBAP2, the last two being aplites) show a characteristic negative Ce anomaly (Ce/Ce*=0.5–0.7; Table 2; Fig. 5a).

In the multi-element spider diagram (Fig. 5b), the samples show enrichment in Rb, Th, U, and K and depletion in Ba, Nb, Sr, P, and Ti. Aplites differ from the other samples, showing markedly lower concentrations in Ba, Rb, and K.

A wide range of bivariate plots (Harker diagrams) were created to study fractionation trends among the observed granitoid rocks. However, most of the major elements showed

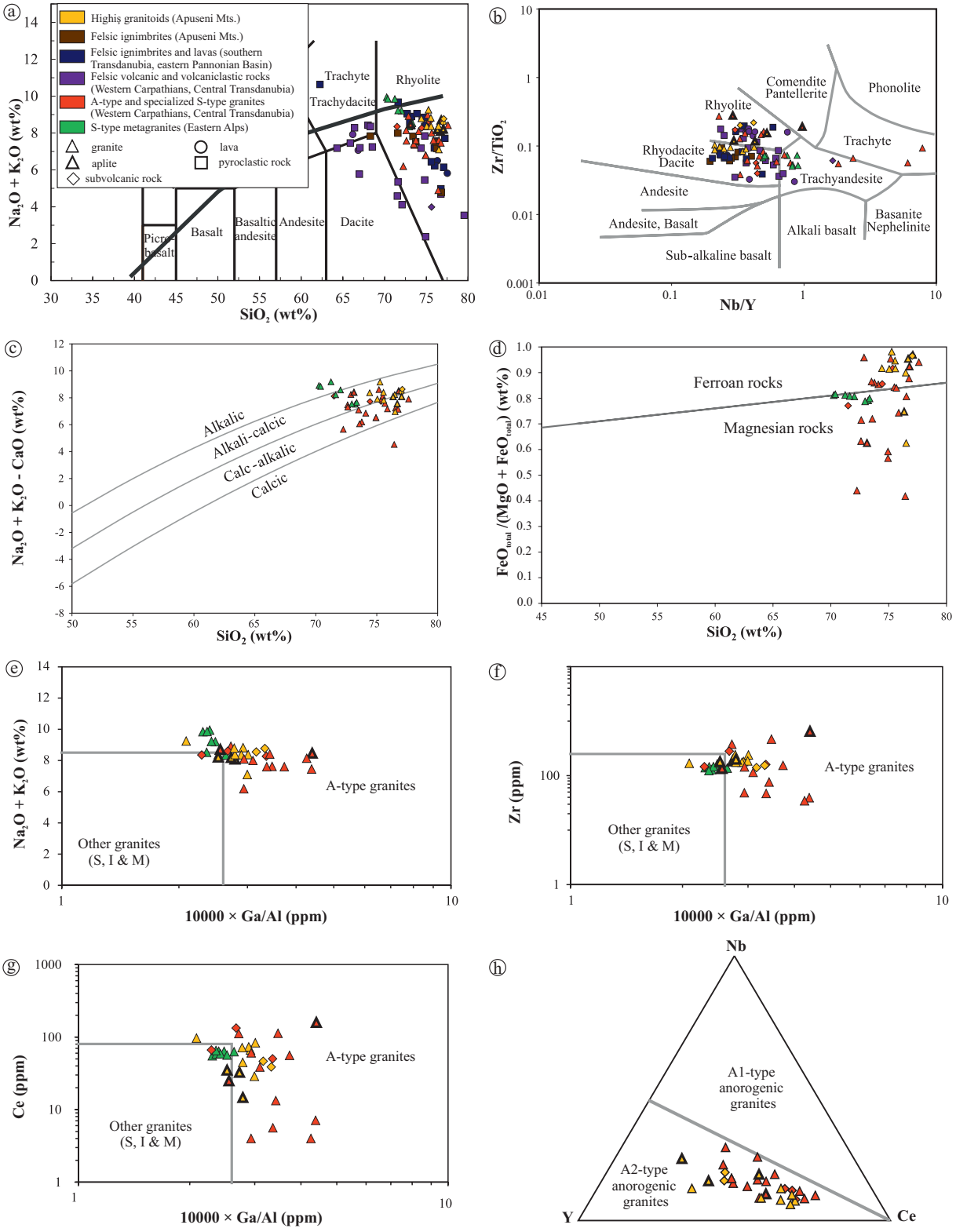

Fig. 3. Whole-rock (major and trace element) geochemistry of the Highiş granitoids and the Permian felsic volcanic rocks in the Tisza Mega-unit (Apuseni Mts., basement of the eastern Pannonian Basin, southern Transdanubia; Nicolae et al. 2014; Szemerédi et al. 2020a), as well as the analogous igneous formations of the ALCAPA Mega-unit (Western Carpathians, Eastern Alps; Uher & Broska 1996; Broska & Uher 2001; Vozárová et al. 2009, 2015, 2016; Kubiš & Broska 2010; Szemerédi et al. 2020a; Yuan et al. 2020). **a** — total alkali-silica diagram (Le Maitre et al. 1989); **b** — Zr/TiO_2 vs. Nb/Y diagram (Winchester & Floyd 1977); **c** — modified alkali-lime index (MALI; Frost et al. 2001); **d** — Fe-number (Frost et al. 2001; Frost & Frost 2008); **e–g** — discrimination diagrams for A-type granitoid rocks (Whalen et al. 1987); **h** — Nb–Y–Ce diagram for the discrimination of A1 and A2 type granitoids (Eby 1992)

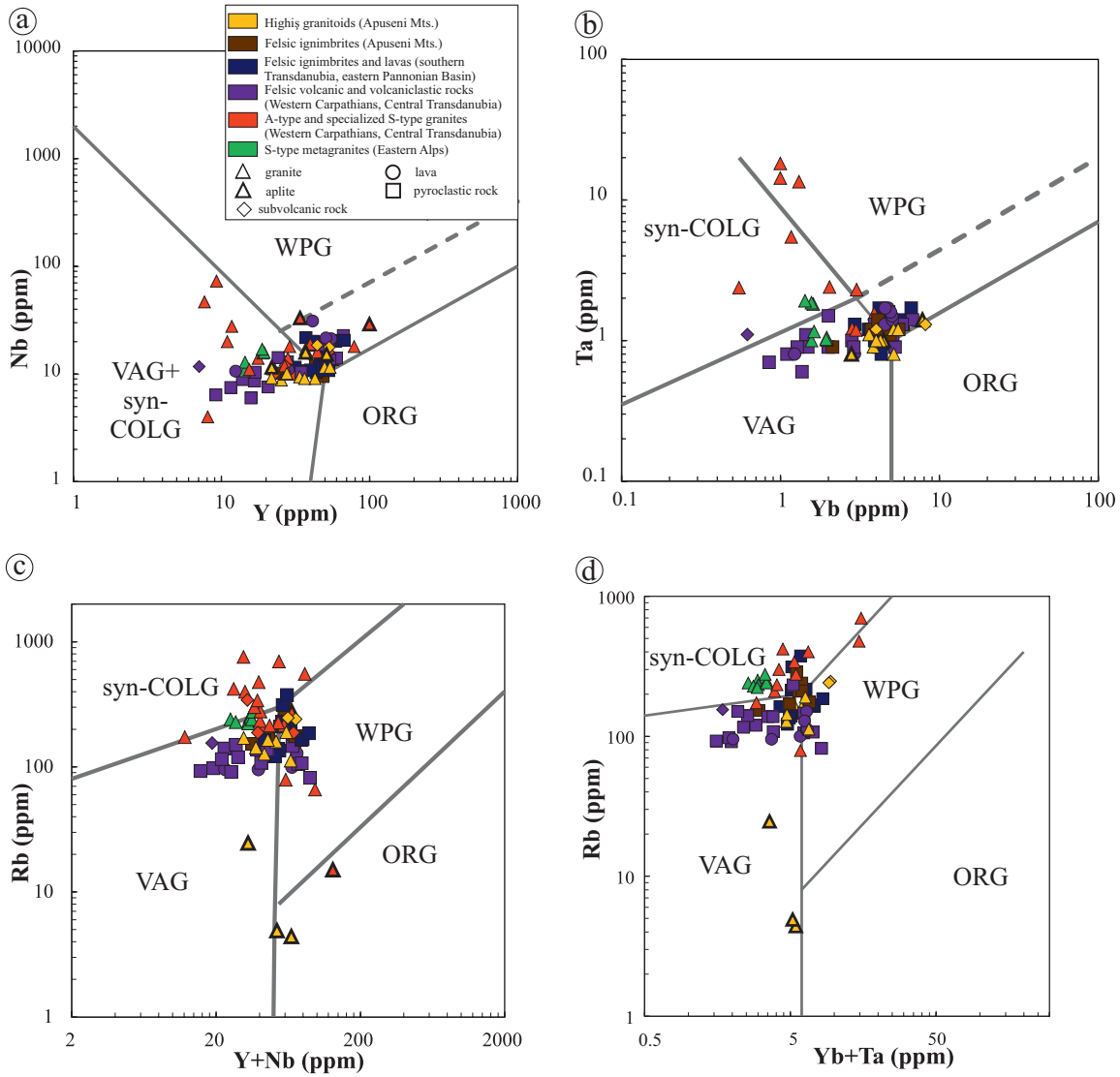

Fig. 4. Y–Nb (**a**), Yb–Ta (**b**), Y+Nb–Rb (**c**), and Yb+Ta–Rb (**d**) diagrams (Pearce et al. 1984) for the geotectonic implications of the studied Permian granitoids in the Apuseni Mts. and the felsic volcanic rocks in the Tisza Mega-unit (Apuseni Mts., basement of the eastern Pannonian Basin, southern Transdanubia). Analogous formations in the ALCAPA Mega-unit (see details in Figs. 1 and 3) were plotted, as well. Abbreviations: ORG=ocean ridge granites, syn-COLG=syn-collision granites, VAG=volcanic-arc granites, WPG=within-plate granites.

very weak (if there any) correlations (R^2=0.0–0.6), suggesting the effects of post-magmatic alteration processes. Relatively immobile Ti (R^2=0.7) is an exception, as well as some trace elements, such as Ba or Sr that show moderate correlations (R^2=0.8).

Based on the method introduced by Boehnke et al. (2013), zircon saturation temperatures were also calculated for the Highiş granitoids (Table 2). Zircon T_{sat} values range between 737 °C and 793 °C, showing slightly lower temperature for microgranites (737–745 °C) and aplites (750–758 °C) than in the case of medium-grained granites (748–793 °C).

Geochronology

Most of the studied zircons are relatively small (100–250 μm), euhedral, bipyramidal, greyish brown crystals. All of them exhibit low-intensity luminescence pattern in CL, showing poorly preserved oscillatory zoning (Fig. 6). The laser ablation spots were placed mostly in the mantle parts of the crystals avoiding cracks, inclusions, or xenocrystic cores. The data give more than 10 % discordance between $^{206}Pb/^{238}U$ and $^{207}Pb/^{235}U$ ages were filtered out (Supplementary Table S1). The remaining $^{206}Pb/^{238}U$ ages give large age ranges suggesting the presence of older (xenocrystic or antecrystic) domains and/or that the zircon crystals do not form closed systems and the pore fluids resulted in selective leaching of mother and daughter isotopes. They have an average 2 s uncertainty between 1.5 and 2.5 %. The average Th/U ratios (0.4–0.5) within samples do not give any systematic relation to the $^{206}Pb/^{238}U$ ages.

We applied the IsoplotR software (Vermeesch 2018) to calculate concordia and weighted mean ages for the studied

samples (Supplementary Fig. S1) and the TuffZirc Age algorithm of ISOPLOT software (Ludwig 2012) on the $^{206}Pb/^{238}U$ ages for selecting the youngest coherent age group of zircon crystals (Fig. 7). From the dates of the TuffZirc age groups weighted mean ages were calculated, as well, including 1.5 % external (systematic) errors. We may consider that these ages reflect the main zircon crystallization period in the granitoid magma batches (Table 3). All of the calculated concordant $^{206}Pb/^{238}U$ ages were examined individually to identify inherited domains and/or zircon crystals affected by Pb-loss.

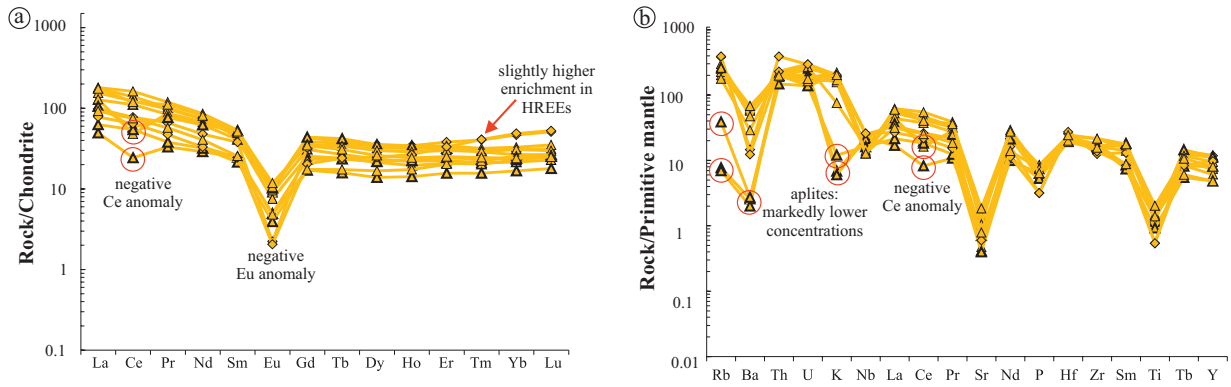

Fig. 5. Chondrite-normalized rare-earth element patterns (**a**) and primitive mantle-normalized spider diagrams (**b**) of the Highiş granitoids (according to Barrat et al. 2012 and Sun & McDonough 1989, respectively).

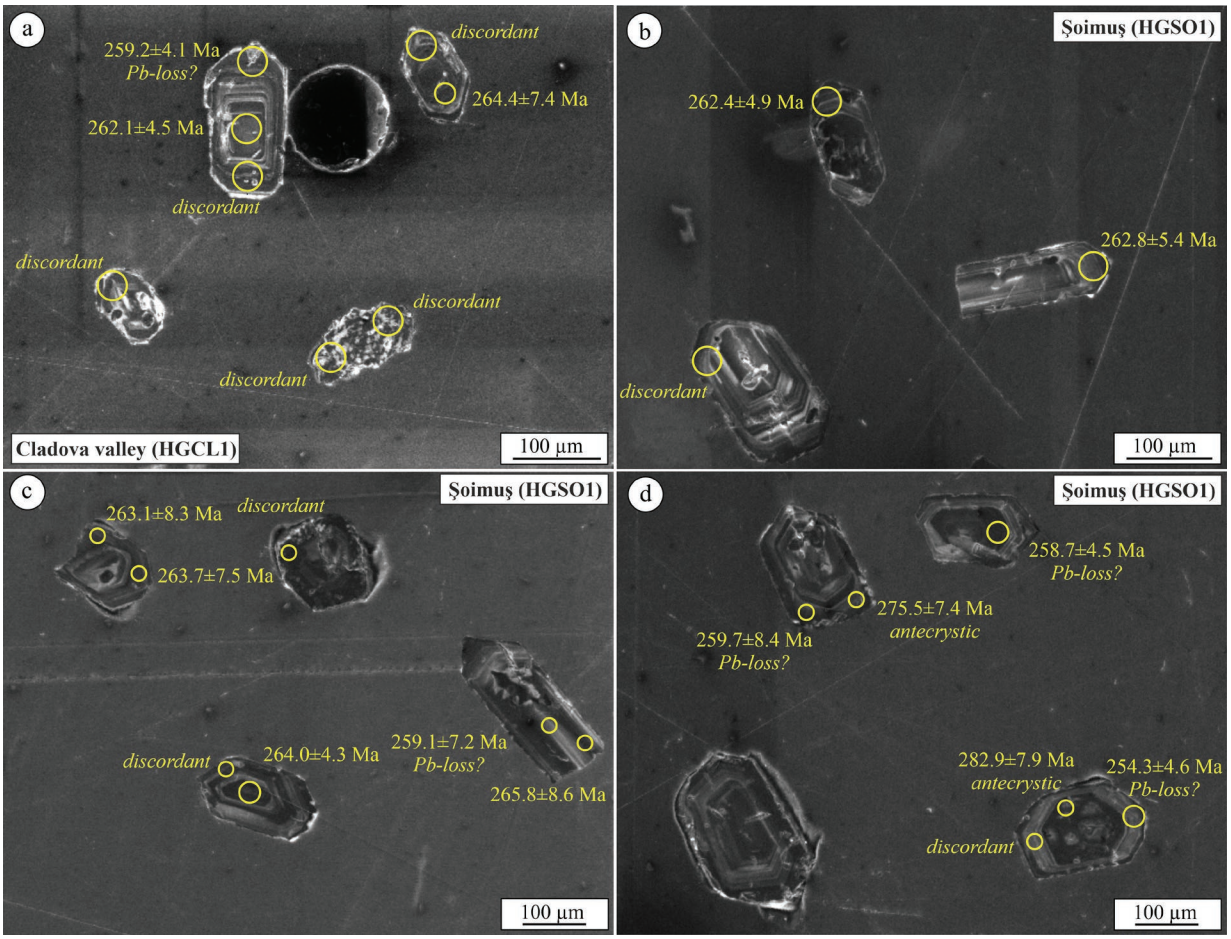

Fig. 6. Cathodoluminescence images of some representative zircon crystals of the Cladova valley (**a**) and the Şoimuş (**b–d**) granitoids, exhibiting all types of spot analyses (concordant, discordant, antecrystic, and possible Pb-loss affected dates). Concordant $^{206}Pb/^{238}U$ dates are given in the figure and all of the single age data are listed in Supplementary Table S1.

From the medium-grained granites of the Baraţca quarry 32 spots were targeted (on 31 zircon crystals) and 16 give concordant dates ranging between 287.8±4.8 Ma and 253.4±3.4 Ma, having a mean Th/U ratio of 0.4±0.1 (1 SD). Concordia age of these (including all of the concordant dates) resulted in 265.3±7.7 Ma with high (7.7) MSWD value (Supplementary Fig. S1), similarly to the weighted mean age of $^{206}Pb/^{238}U$ dates (264.5±3.6 Ma; MSWD=11.4), both suggesting multiple age components. Ten dates comprise the youngest coherent age group with a TuffZirc age of 267.6+2.3–3.4 Ma (Fig. 7). The <260 Ma four dates may be affected by Pb-loss or represent the ultimate phase of zircon crystallization in the magma reservoir, while the oldest two dates could be interpreted as xenocrystic or antecrystic domains. The dates of the TuffZirc age group represent the main zircon crystallization period with a weighted mean age of 267.8±4.4 Ma including 1.5 % external (systematic) errors (MSWD=1.7).

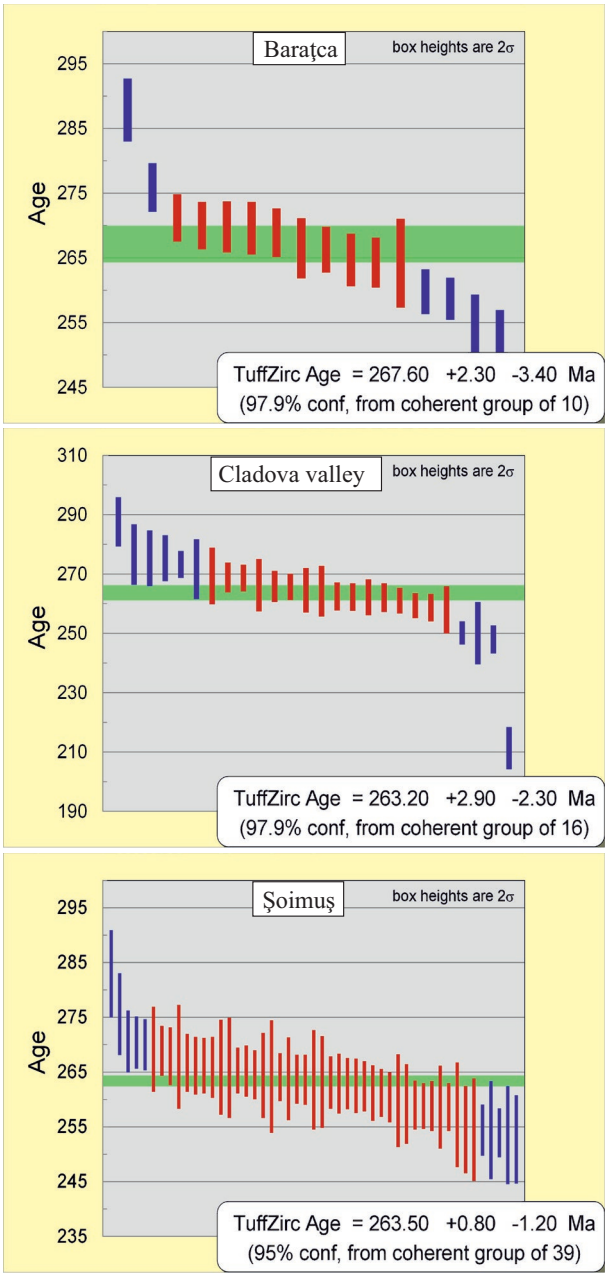

Fig. 7. Results of the zircon U–Pb geochronology of the studied Permian granitoid rocks (medium-grained, equigranular granites; Baraţca: HGBC1, Cladova valley: HGCL1; Şoimuş: HGSO1) in the Apuseni Mts. The TuffZirc Age algorithm (Ludwig 2012) was applied to identify the mean age of the youngest coherent age component

From the Cladova valley outcrop (Fig. 6a), 26 zircon spots out of the 47 (on 20 crystals) give concordant dates ranging between 287.5±8.2 Ma and 211.1±7.0 Ma with mean Th/U ratio of 0.5±0.2 (1 SD). Concordia age calculations (including all of the concordant dates) resulted in 261.1±8.9 Ma with high (8.3) MSWD value (Supplementary Fig. S1), while the calculated weighted mean age of the $^{206}Pb/^{238}U$ dates is 262.4±3.2 Ma (MSWD=8.2). Sixteen dates comprise the youngest coherent age group with a TuffZirc age of 263.2+2.9–2.3 Ma (Fig. 7). The <260 Ma seven dates may be affected by Pb-loss or refer to the ultimate phase of zircon crystallization, while two older dates could be interpreted as xenocrystic or antecrystic domains (287.5±8.2 Ma and 276.4±10.1 Ma). The main zircon crystallization period in this magmatic system might be represented by the weighted mean age of 263.2±4.4 Ma including 1.5 % external (systematic) errors (MSWD=1.8).

In the Şoimuş quarry (Fig. 6b–d), 50 spot analyses prove to be concordant out of the 65 analyzed (on 50 crystals) ranging between 519.6±8.4 Ma and 252.6±8.0 Ma and having a 0.5±0.1 (1 SD) average Th/U ratio. The abovementioned older, xenocrystic date (519.6±8.4 Ma) was ruled out of all calculations and the other two dates were supposed to represent antecrystic domains, as well (282.9±7.9 and 275.5±7.4 Ma; Fig. 6d). Concordia age of these (including all of the concordant dates) resulted in 264.5±32.1 Ma with high (42) MSWD value (Supplementary Fig. S1), similarly to the weighted mean age of $^{206}Pb/^{238}U$ dates (262.2±1.5 Ma; MSWD=3.6). Ruling out xenocrystic and antecrystic dates, concordia age calculations resulted in 261.9±1.1 Ma (MSWD=1.4), while the weighted mean age is similarly 261.9±1.3 Ma (MSWD=2.8). Thirty-nine dates comprise the youngest coherent age group with a TuffZirc age of 263.5+0.8–1.2 Ma (Fig. 7). The <260 Ma fifteen dates may be affected by Pb-loss or belong to the last phase of zircon crystallization in the system. The dates of the TuffZirc age group represent the main zircon crystallization period with a weighted mean age of 262.9±4.1 Ma including 1.5 % external (systematic) errors (MSWD=1.4).

Discussion

Permian felsic magmatic rocks in the Tisza Mega-unit: possible connections of the Highiş granitoids

The petrography of the Highiş granitoids reveals that they have syenogranitic to alkali-feldspar granitic modal compo-

Table 3: Compilation of the zircon in-situ geochronological results obtained from the Permian Highiş granitoids, Apuseni Mts.

Sample	HGBC1	HGCL1	HGSO1
Locality	Barațca	Cladova valley	Şoimuş
Concordant/all spots	16/32	26/47	50/65
Xenocrystic/antecrystic domains	2	2	3
Possible Pb-loss (<260 Ma)	4	7	15
Th/U (1 SD)	0.4±0.1	0.5±0.2	0.5±0.1
TuffZirc age (Ma)	267.6+2.3–3.4 (10)	263.2+2.9–2.3 (16)	263.5+0.8–1.2 (39)
Weighted mean age (Ma)	267.8±4.4	263.2±4.4	262.9±4.1

sitions (Table 1). The rock-forming mineral assemblage is composed of varying amounts of K-feldspar (orthoclase and microcline), quartz, plagioclase (albite), and biotite. Secondary minerals are unambiguously represented by muscovite. Based on the results of the whole-rock chemical analyses, the studied samples plot into the granite and granodiorite fields. Generally, they are subalkaline, slightly peraluminous and have an alkali-calcic or calc-alkalic character (Fig. 3). Mineralogical and geochemical features of the Highiş granitoids reflect their A-type affinity based on our data (e.g. presence of Fe-rich biotite, ferroan character, binary plots using trace Ga content, moderate to high ΣREE content, and seagull-shaped REE patterns with pronounced negative Eu anomaly) and those previously published by Bonin & Tatu (2016). These authors reported that biotite is iron-rich in the felsic rocks of the Highiş massif, corresponding to the annite composition.

It is widely accepted that the characteristic 'seagull' REE pattern refers to hot-dry-reduced magmas formed in the areas of mantle-upwelling (hotspots or continental rifts; Christiansen 2005; Bachmann & Bergantz 2008; Christiansen & McCurry 2008; Ondrejka et al. 2021). Relatively high Zr-saturation temperature (737–793 °C; according to the thermometer of Boehnke et al. 2013) also indicates crystallization from mild- to moderately high-temperature and dry magma. Furthermore, the geotectonic diagrams of Pearce et al. (1984) can also support the anorogenic (A-type) character of the Highiş granitoid rocks that are often (but not necessarily) related to a post-collisional to extensional environment (Fig. 4). Therefore, the proposed tectonic setting fits well into the post-orogenic rifting of the Paleo-Tethyan realm during Late Paleozoic times (e.g. Uher & Broska 1996; Putiš et al. 2000; Broska & Uher 2001; Stampfli & Kozur 2006; Bonin 2007).

On the other hand, the whole-rock chemical composition of the studied granitoids was plotted with the Permian felsic volcanic rocks of the Tisza Mega-unit (Apuseni Mts., basement of the eastern Pannonian Basin, southern Transdanubia; Nicolae et al. 2014; Szemerédi et al. 2020a) for comparison (Figs. 3, 4, 8, and 9). Both plutonic and volcanic rocks have similar geochemistry and zircon ages, suggesting a Mid-Permian (~270–260 Ma) magmatic event (Table 3 and Szemerédi et al. 2020a), thus indicating a common or similar source and geotectonic setting. Their feasible genetic connection is also supported by the La_N vs. La_N/Yb_N diagram (Fig. 8f) that shows a positive linear trend for all of the studied Permian felsic magmatic rocks (A-type Highiş granitoids, Apuseni ignimbrites, and felsic volcanic rocks from Hungary).

Permian plutonic–volcanic connections: a working hypothesis

Although the new zircon U–Pb dates of medium-grained granites are often discordant and concordant dates show high MSWD values, they most commonly belong to the Guadalupian (270–260 Ma) period. The high MSWD values and the frequency of discordant dates might derive from (1) the high U content and alpha-damage density of the zircon crystals, (2) the presence of unobserved inclusions and/or (3) secondary processes that might affect isotope ratios of the analyzed grains as discussed in detail below.

Concordant age data (Table 3) correspond well to the radiometric age obtained by Pană et al. (2002) from the porphyritic microgranite (Jernova quarry: 264.2±2.3 Ma). The calculated main zircon crystallization ages (Barațca: 267.8±4.4 Ma, Cladova valley: 263.2±4.4 Ma, and Şoimuş quarries: 262.9±4.1 Ma) fall perfectly within the timespan of the Permian silicic volcanic activity in the Tisza Mega-unit (~267–260 Ma; Fig. 10) that is based on the zircon geochronology of five pyroclastic/lava samples from southern Transdanubia and the basement of the eastern Pannonian Basin (Szemerédi et al. 2020a). All of these data suggest a relatively short (≤10 Ma), Mid-Permian magmatic event in the Tisza Mega-unit that was associated with a post-collisional extensional tectonic regime (most likely continental rifting; Fig. 4). It is important to note that monazite datings of the Permian felsic volcanic and volcaniclastic rocks in the Dacia Mega-unit (Sirinia Basin, Southern Carpathians; Fig. 1a) revealed significantly older (Early Permian: 296±3.2 Ma; Fig. 10; Kędzior et al. 2020) ages than those of the Highiş granitoids.

Based on Sr–Nd isotope geochemistry of the Apuseni ignimbrites, Nicolae et al. (2014) proposed the generation of the felsic melt within the lower crust due to the emplacement of mantle-derived mafic magmas that provided heat leading to partial melting. Continental crustal source and partial melting could be supported by major and trace element geochemistry including the discrimination system of Eby (1992), according to which all of the studied Permian felsic rocks are A2-type (Fig. 3h).

It can be assumed that plutonic and volcanic rocks with very similar major and trace element compositions, as well as zircon U–Pb ages refer to compositionally similar, crystal-rich granodioritic magma batches. Some of the magma batches developed at shallow crustal levels might have been rejuvenated and erupted during the Mid-Permian, producing a large

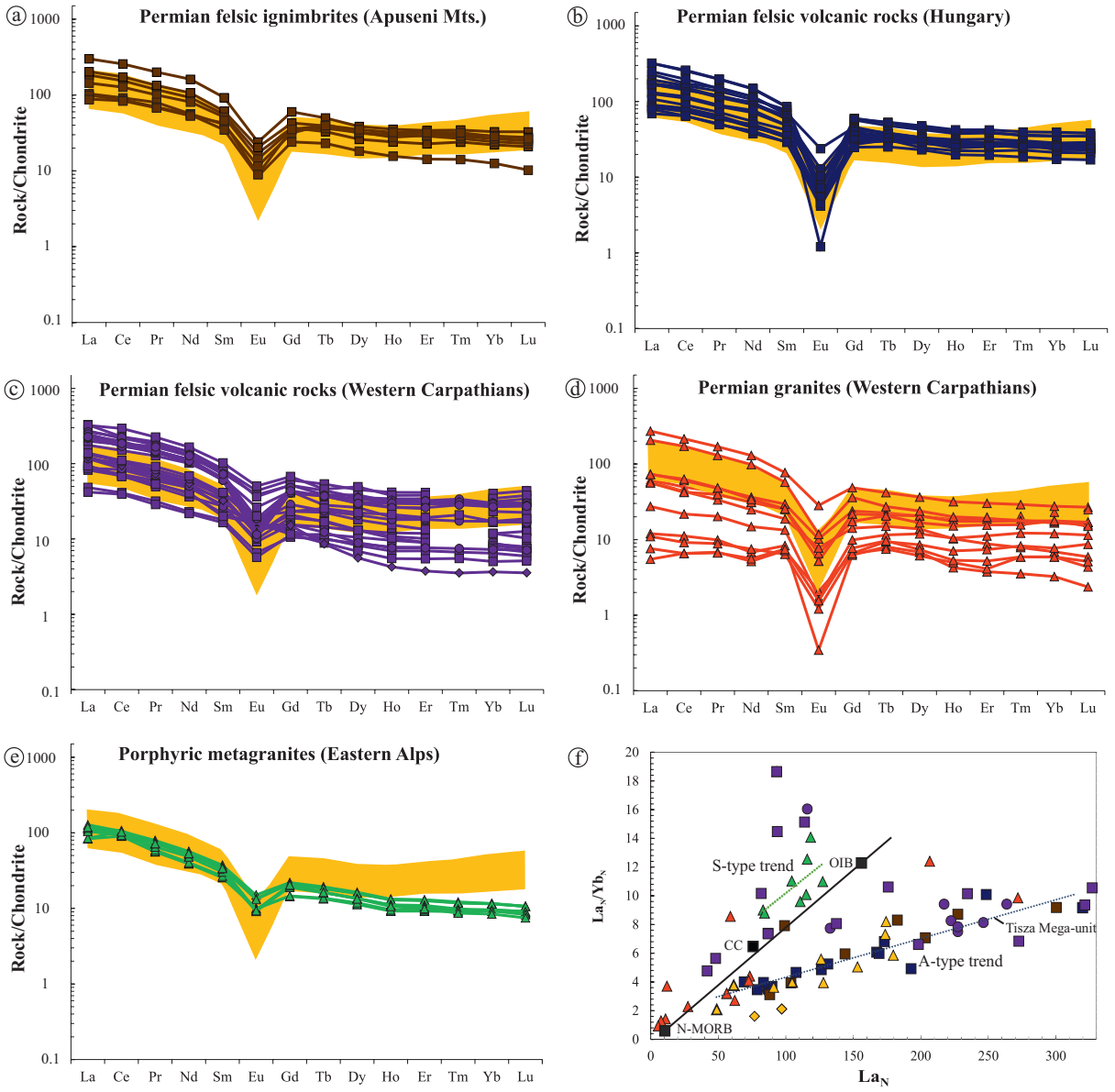

Fig. 8. Chondrite-normalized (Barrat et al. 2012) rare-earth element patterns comparing the Highiş granitoids (yellow area in the background, omitting samples with negative Ce anomaly) to the Permian felsic ignimbrites in the Apuseni Mts. (**a**; Nicolae et al. 2014); Permian felsic volcanic rocks in the basement of the eastern Pannonian Basin and southern Transdanubia (**b**; Szemerédi et al. 2020a); Permian to Triassic felsic volcanic rocks in the Western Carpathians and Central Transdanubia (**c**; Vozárová et al. 2009, 2015, 2016; Kubiš & Broska 2010; Szemerédi et al. 2020a); Permian to Triassic A-type and specialized S-type granites in the Western Carpathians and the Velence Mts. (**d**; Broska & Uher 2001; Kubiš & Broska 2010); Permian porphyric metagranites in the Eastern Alps (**e**; Yuan et al. 2020). All of the aforementioned samples were plotted in the the La_N/Yb_N vs. La_N diagram (**f**). Abbreviations: N-MORB=Mid Ocean Ridge Basalt (Sun & McDonough 1989), OIB=Ocean Island Basalt (Sun & McDonough 1989), CC=average continental crust (Rudnick & Gao 2003). Symbols are the same as those in Figures 1, 3, and 4.

volume of the crystal-rich rhyodacitic/dacitic pyroclastic rocks that are widespread in the Tisza Mega-unit (Nicolae et al. 2014; Szemerédi et al. 2016, 2017, 2020a,b), while others probably crystallized at crustal depths as intermediate plutons. Zircon crystals refer to the approximate time of the plutonism, however, the complete crystallization of such magma batches might have occurred hundreds of thousands to millions of years later than the obtained zircon radiometric ages. The youngest concordant dates between 259.7±3.4 and 247.8±4.6 Ma could represent the ultimate phase of zircon crystallization in the magma reservoir or can refer to the effects of Pb-loss.

Despite the fact that major element compositions and the mineral assemblages refer to granitic (rhyolitic) plutonic and volcanic rocks (Szemerédi et al. 2016, 2017, 2020a,b), true granites (rhyolites), according to the trace elements, are subordinate (Fig. 3b). Small batches of true rhyolitic melts might have fractionated from some of these crystal-rich granodioritic magma reservoirs and crystallized at shallower depths as

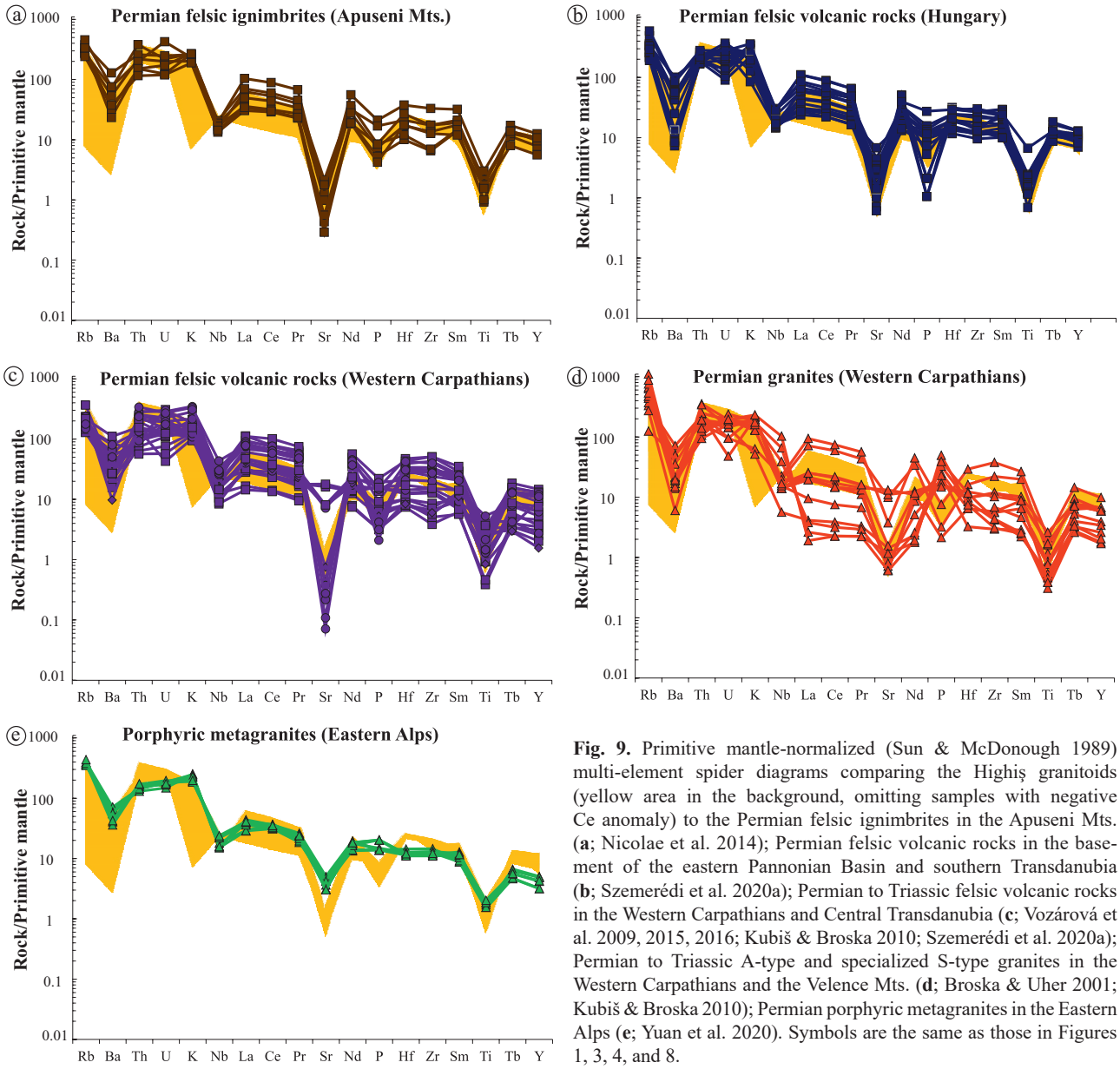

Fig. 9. Primitive mantle-normalized (Sun & McDonough 1989) multi-element spider diagrams comparing the Highiş granitoids (yellow area in the background, omitting samples with negative Ce anomaly) to the Permian felsic ignimbrites in the Apuseni Mts. (**a**; Nicolae et al. 2014); Permian felsic volcanic rocks in the basement of the eastern Pannonian Basin and southern Transdanubia (**b**; Szemerédi et al. 2020a); Permian to Triassic felsic volcanic rocks in the Western Carpathians and Central Transdanubia (**c**; Vozárová et al. 2009, 2015, 2016; Kubiš & Broska 2010; Szemerédi et al. 2020a); Permian to Triassic A-type and specialized S-type granites in the Western Carpathians and the Velence Mts. (**d**; Broska & Uher 2001; Kubiš & Broska 2010); Permian porphyric metagranites in the Eastern Alps (**e**; Yuan et al. 2020). Symbols are the same as those in Figures 1, 3, 4, and 8.

aplites or microgranites that show granitic (rhyolitic) compositions (Fig. 3b), slightly lower zircon saturation temperatures (Table 2) and slightly differ from the medium-grained granitoids in their REE and other immobile trace element patterns (Fig. 5). Permian volcanic rocks with rhyolitic composition are also relatively rare in the Tisza Mega-unit and represent only one area of the eastern Pannonian Basin, the Battonya–Pusztaföldvár Basement Ridge (Fig. 1a; Szemerédi et al. 2020b).

Voluminous, pyroclastic eruptions of the crystal-rich magma batches were most possibly led by mantle-derived mafic magma influxes that provided sufficient heat and rejuvenated the felsic crystal mushes (e.g. Annen et al. 2006). Permian mafic-intermediate lavas occur in the Codru-Moma Mts. (Fig. 1b) forming a bimodal volcanic suite with the felsic ignimbrites (Nicolae et al. 2014). Similarly, gabbros and diorites are also associated with the Highiş granitoids within the Highiş igneous complex (SW Apuseni Mts.; Pană et al. 2002; Bonin & Tatu 2016). It is feasible to assume that all of these mafic to felsic plutonic and volcanic rocks represent a large cogenetic plutonic–volcanic complex similar to the short-lived (5–10 Myr) Early Permian bimodal Sesia Magmatic System in the Southern Alps of Italy (Sinigoi et al. 2010; Karakas et al. 2019; Tavazzani et al. 2020). However, the exploration of this Mid-Permian magmatic system requires further research, including the radiometric age dating and whole-rock geochemical analyses of mafic–intermediate plutonic and volcanic rocks, as well as the isotope geochemistry of the whole igneous complex.

Permian plutonic–volcanic connections between the Highiş granitoids (Biharia Nappe System) and the felsic volcanic rocks of the Tisza Mega-unit suggest that the Biharia Nappe

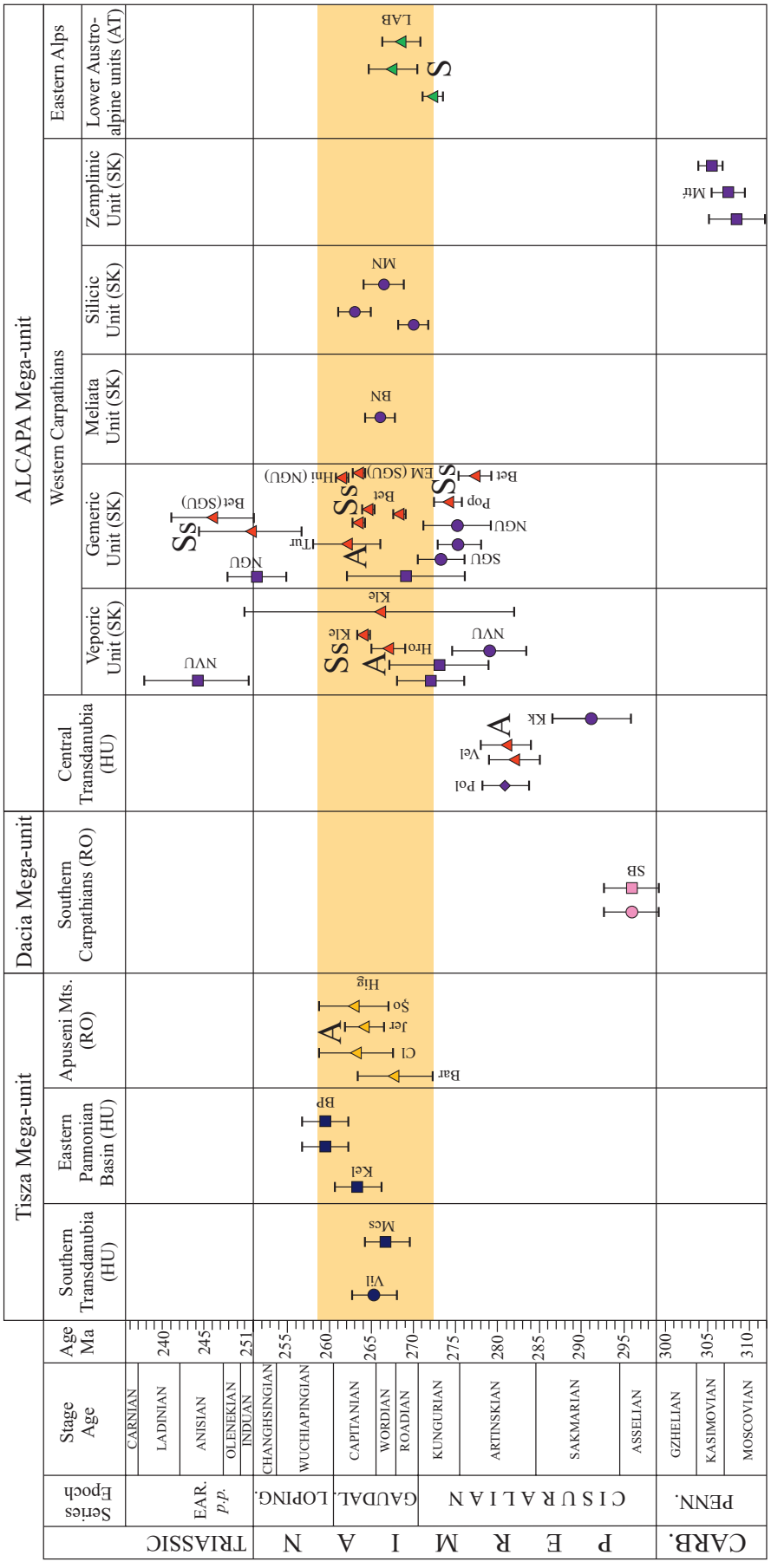

Fig. 10. Zircon (and monazite) U–Pb age data of the studied Permian granitoid rocks in the SW Apuseni Mts. (weighted mean ages calculated by the dates of the TuffZirc age groups) and the felsic volcanic rocks in the Tisza Mega-unit (basement of the eastern Pannonian Basin, southern Transdanubia), as well as the analogous igneous formations of the ALCAPA Mega-unit (Western Carpathians, Eastern Alps; Pană et al. 2002; Hraško et al. 2002; Poller et al. 2002; Lelkes-Felvári & Klötzli 2004; Radvanec et al. 2009; Uher & Ondrejka 2009; Vozárová et al. 2009, 2012, 2015, 2016, 2018; Kubiš & Broska 2010; Ondrejka et al. 2018, 2021; Kędzior et al. 2020; Szemerédi et al. 2020a; Yuan et al. 2020; Villaseñor et al. 2021). Symbols are the same as those in Figures 1, 3, 4, 8, and 9. Abbreviations: Bar=Baraţca, BP=Battonya–Pusztaföldvár Basement Ridge, Bet=Betliar, BN=Bôrka Nappe, Cl=Cladova valley, EM=Elisabeth Mine, Hig=Highiş massif, Hni=Hlinec, Hro=Hrončok, Jer=Jernova, Kel=Kelebia area, Kk=Kékkút, Kle=Klenovec, LAB=Lower Austroalpine basement, Mcs=Western Mecsek Mts., MN=Muraň Nappe, Mtí=Malá Tŕňa, Pol=Polgárdi, Pop=Poproč, NGU=Northern Gemeric Unit, NVU=Northern Veporic Unit, SB=Sirinia Basin, SGU=Southern Gemeric Unit, Şo=Şoimuş, Tur=Turčok, Vel=Velence Mts., Vil=northern foreland of the Villány Mts., A=A-type, S=S-type, Ss=specialized S-type granitoids.

System might belong to the Tisza Mega-unit, as well. The latter is in contradiction with the tectonic models of Schmid et al. (2008, 2020), considering the Biharia Nappe System as part of the Dacia Mega-unit; however, it supports the model previously introduced by Csontos & Vörös (2004).

Regarding plutonic–volcanic connections, two different approaches were raised in the last decades. (1) According to the so-called 'crystal mush model' (e.g. Bachmann & Bergantz 2004, 2008; Hildreth 2004; Bachmann et al. 2007) high-silica melts are generated by extraction from shallow crystal mushes (50–60 vol. % crystallinity) that freeze as an intermediate pluton. Such separation of the eruptible melt should lead to compositional differences between volcanic rocks and intermediate plutons (left behind as cumulate residues) in general.

On the other hand, (2) Glazner et al. (2015), using global geochemical databases for plutonic and volcanic rocks (circum-Pacific convergent margins and western North America), found little evidence for loss of liquid from plutons. As the trace element patterns studied by them proved to be generally indistinguishable between plutonic and the associated volcanic samples, they suggested that liquids fractionated from crystal-rich felsic magmas are of relatively small volume and immobile (e.g. aplites; Glazner et al. 2008, 2015). Their trace element geochemical observations were supported by zircon U–Pb geochronological data, as well. Taking into consideration the strongly similar whole-rock compositions and the indistinguishable zircon ages of the Permian felsic plutonic rocks and the felsic (rhyodacitic/dacitic to rhyolitic) ignimbrites and lavas in the Tisza Mega-unit, our study corresponds better to the approach of Glazner et al. (2008, 2015), suggesting similar crustal sources and igneous processes in the case of most of the studied felsic rock types.

Closed versus open systems: nature of the alteration processes

Some mineralogical and bulk geochemical signatures such as the subordinate presence of secondary muscovite together with sericitization of feldspars, weak correlations of the major elements, slightly scattered A/NK and A/CNK values (Table 2), contradictory rock classifications (Fig. 3a,b), and the slightly scattered Ce content (Table 2; Fig. 5) indicate the contribution of the post-emplacement alteration processes to the evolution of the studied Permian Highiș granitoids.

Based on the study of Cl-rich hydrous mafic mineral assemblages in the Highiș igneous complex, Bonin & Tatu (2016) proved that the A-type felsic rocks are compositionally complex. Among the rock-forming minerals, the Fe-rich biotite which occurs as small aggregates could replace primary amphibole. Microcline, albite, and muscovite also appear as secondary minerals in the A-type alkali-feldspar granite, and albite granite derived from hydrothermal alteration processes (e.g. Na- and K-metasomatism).

It is noteworthy, that the first halogen-rich hydrothermal episode took place more likely by fluid exsolution shortly after Mid-Permian emplacement and during cooling (Bonin & Tatu 2016). Subsequently, the rocks of the igneous massif were overprinted by shearing and retrograde metamorphic events which were accompanied by an influx of fluids that produced alteration assemblages indicating upper greenschist facies conditions (>400 °C; Ciobanu et al. 2006; Bonin & Tatu 2016). Related data point to fluids percolating through fractures and shear zones and pervasively penetrating the whole Highiș igneous complex during hydrothermal episodes that would have occurred from the Mid-Permian (e.g. halogen-rich fluids; Bonin & Tatu 2016) to the Mid-Cretaceous (e.g. neutral low reducing fluids; Ciobanu et al. 2006).

It was revealed that the Permian felsic volcanic rocks in the Tisza Mega-unit were also affected by various post-magmatic alterations, including Na- and/or K-metasomatism, hydrothermal alterations, and locally Alpine low-grade metamorphism (Nicolae et al. 2014; Szemerédi et al. 2020a). In general, these processes could influence the distribution of the fluid-mobile element concentrations as discussed by Szemerédi et al. (2020a). With respect to the less mobile elements, including REE, U, Th, Y, and Zr, a local mobilization effect of F-rich hydrothermal solutions was also suggested in some outlier samples that were manifested by extremely low immobile trace-element compositions. Such bulk geochemical features, however, are not observed in the present study regarding Highiș granitoids, reflecting dominantly closed system modifications.

Nevertheless, some granitoid samples (mostly aplites) show systematic depletion in Ce with respect to the chondrite composition (Fig. 5a), presumably due to the selective leaching of this element. Cerium, unlike the other REEs, exists in 3+ or 4+ oxidation states and their fractionations can be related to the changes of the redox conditions (e.g. McLennan 1989). Various processes are able to generate a negative Ce anomaly, for example, such a feature was observed in volcanic arc suites where its origin was attributed to the addition of sedimentary component to the magma source (Bellot et al. 2018). Additionally, negative Ce anomalies can result from several secondary processes such as tropical weathering and hydrothermal alterations (Bellot et al. 2018 and references therein). The relationship between the geotectonic setting of the study area and the previously published nature of the alteration events (Ciobanu et al. 2006; Bonin & Tatu 2016) suggest that mobilization effect of shearing episodes can be accounted for the observed negative Ce anomaly. Therefore, hydrothermal fluids could preferentially scavenge granite-related Ce^{4+} relative to other trivalent REEs. Such changes could be supported by the precipitation of Ce-rich minerals from epidote-bearing veins in the Highiș massif (Ciobanu et al. 2006). Based on their mineralogical data from the main vein prospect in the igneous suite (Șoimuș Ilii), epidote shows significant REE-enrichment towards allanite-(Ce); furthermore, the presence of monazite-(Ce) was also documented. Notice that the cores of zoned epidote crystals can have Ce_2O_3 concentrations as high as 6.5 wt. %.

With respect to the high MSWD values of concordant zircon U–Pb dates and the frequency of discordant dates, the aforementioned shearing processes and the Alpine hydrothermal

events could also overprint the original isotopic record (e.g. Pb-loss). Nevertheless, the observed Th/U ratios of the zircon crystals provided concordant dates that are normal magmatic. This feature together with the documented texture of the analyzed zircon crystals highlights that the aforementioned mobilization effect seems to be negligible regarding precise dating of the investigated Permian magmatic event.

Regional correlation of the Highiş granitoids and the Permian felsic volcanic rocks in the Tisza Mega-unit

Due to the Europe-derived nature of the Tisza Mega-unit (e.g. Haas et al. 1999; Szederkényi et al. 2013a), we started the geochronological and geochemical comparison of the studied rocks with the similar formations in the Central European Variscides that represent the stable European plate (Bohemian Massif). However, this study, completing our previous results of the Permian felsic volcanic rocks in the Tisza Mega-unit (Szemerédi et al. 2020a), revealed that the studied silicic magmatism was a Mid-Permian (~270–260 Ma) event, significantly younger than the similar magmatic episodes within the European plate (e.g. in the Southern Permian or the Intra-Sudetic Basins) that occurred in the Latest Carboniferous to Earliest Permian times (300–290 Ma; Breitkreuz & Kennedy 1999; Awdankiewicz & Kryza 2010; Repstock et al. 2017; Słodczyk et al. 2018; Lützner et al. 2021).

Therefore, we tried to find analogous formations with similar radiometric ages and/or geochemical characteristics in other areas, including the Alpine–Carpathian–Pannonian region (ALCAPA Mega-unit; Fig. 1a). Despite the fact that the latter represents a composite terrane having different evolution from the Tisza Mega-unit, it bears the signs of several Permo-Carboniferous to Lower Triassic magmatic episodes that seemed to be worth comparing with the studied one (Uher & Broska 1996; Petrík & Kohút 1997; Broska & Uher 2001; Poller et al. 2002; Vozárová et al. 2009, 2012, 2015, 2016, 2018; Kubiš & Broska 2010; Ondrejka et al. 2018, 2021; Szemerédi et al. 2020a; Yuan et al. 2020; Villaseñor et al. 2021). We tried to collect all the available whole-rock geochemical (Uher & Broska 1996; Broska & Uher 2001; Vozárová et al. 2009, 2015, 2016; Kubiš & Broska 2010; Yuan et al. 2020) and zircon (or monazite) geochronological (e.g. Hraško et al. 2002; Poller et al. 2002; Lelkes-Felvári & Klötzli 2004; Rojkovič & Konečný 2005; Vozárová et al. 2009, 2012, 2015, 2016, 2017, 2018, 2019; Kubiš & Broska 2010; Radvanec et al. 2009; Uher & Ondrejka 2009; Ondrejka et al. 2018, 2021; Yuan et al. 2020, Villaseñor et al. 2021) data of the ALCAPA Mega-unit (the Western Carpathians, Central Transdanubia, and the Eastern Alps; Fig. 1a) and properly compare them to those of the Highiş granitoids and the associated Permian felsic volcanic rocks (Pană et al. 2002; Nicolae et al. 2014; Szemerédi et al. 2020a; Fig. 1a–b).

In the Western Carpathians, four major groups of Variscan collisional (orogenic) to post-collisional extensional (post-orogenic) granites occur (S, I, A, and specialized S-type; Broska & Uher 2001), among which post-orogenic A-type and specialized S-type granites are Permo-Triassic in age (Poller et al. 2002; Radvanec et al. 2009; Uher & Ondrejka 2009; Kubiš & Broska 2010; Ondrejka et al. 2021; Villaseñor et al. 2021), representing the Gemeric and the Veporic Units, the Pieniny Klippen Belt, as well as Central Transdanubia (Velence Mts.; Fig. 1a). Permo-Carboniferous felsic pyroclastic rocks, lavas, and dykes are also widespread within the aforementioned crustal-scale superunits of the Western Carpathians (Vozárová et al. 2009, 2015, 2016) as well as in the Silicic (Ondrejka et al. 2018), Meliata (Vozárová et al. 2012) and Zemplinic (Vozárová et al. 2018) Units and appear at the Kékkút and Polgárdi localities in Central Transdanubia, as well (Lelkes-Felvári & Klötzli 2004; Szemerédi et al. 2020a; Fig. 1a). All of these Permian felsic plutonic and volcanic formations were compared to the studied samples in the geochemical diagrams (Figs. 3a–f, 4, 8, 9) and the geochronological timescale (Fig. 10). Moreover, porphyric metagranites, showing similar, Mid-Permian zircon ages, from the Eastern Alps (Lower Austroalpine units; Yuan et al. 2020) were involved in the comparison because of their relative vicinity (Fig. 1a).

As post-magmatic alterations (e.g. low-grade metamorphism, K-metasomatism, hydrothermal alteration) often affected the multi-elemental composition of the Western Carpathian igneous rocks, as well (e.g. Poller et al. 2002; Rojkovič & Konečný 2005; Vozárová et al. 2009, 2015; Kubiš & Broska 2010), the geochemical comparison was based on relatively immobile trace elements. In the REE (Fig. 8d) and multi-element spider diagrams (Fig. 9d) Permian to Triassic granitoid rocks of the Western Carpathians show diverse, but in many cases similar, parallel patterns with the studied Permian felsic plutonic and volcanic rocks in the Tisza Mega-unit (Figs. 8a–b and 9a–b). However, this similarity, supported by the trend of REE fractionation (Fig. 8f), as well, dominantly belongs to the A-type granites (Velence Mts., Veporic Unit, and Pieniny Klippen Belt; Broska & Uher 2001; Fig. 1a), while the specialized S-type granites in the Gemeric Unit (Broska & Uher 2001; Kubiš & Broska 2010; Villaseñor et al. 2021) significantly differ in trace element composition. Although, according to the radiometric datings of the last two decades, Western Carpathian A-type and specialized S-type granites proved to be significantly older (Cisuralian: ~281–275 Ma) or younger (Lower Triassic: ~251–239 Ma) than the studied felsic rocks in the Tisza Mega-unit, recent studies revealed Mid-Permian magmatic episodes in that region, too. Specialized S-type granites in the Gemeric and Veporic Units yielded 265–264 Ma dominant zircon crystallization ages (Villaseñor et al. 2021), while A-type granites in the Central Western Carpathians (Hroncok, Turcok, and Upohlav occurrences) gave the age of 267–262 Ma, only granitoid rocks in the Velence Mts. proved to be older having an age of 281 Ma (Ondrejka et al. 2021). Despite the similar Mid-Permian ages, only the A-type granites of the Western Carpathians showed geochemical similarity to the Highiş granitoids.

Regarding the trace element compositions, a similar dichotomy was observed between the Permian felsic volcanic rocks

in the Western Carpathians and the studied rocks. Felsic pyroclastic rocks, lavas, and dykes (Gemeric and Veporic Units, Central Transdanubia; Vozárová et al. 2009, 2015, 2016; Szemerédi et al. 2020a; Fig. 1a) can be divided into two major groups. One of them consists of felsic volcanic rocks with A-type character that show similar, parallel REE and other immobile element patterns (Figs. 8c, f and 9c) with the samples of the Tisza Mega-unit. This group basically includes lavas from the Southern Gemeric Unit (Vozárová et al. 2009) and some pyroclastic rocks from the Northern Gemeric Unit (Vozárová et al. 2015) that plot perfectly in the positive linear trend defined by the studied Permian felsic rocks in the Tisza Mega-unit (Fig. 8f). On the other hand, S-type felsic volcanic rocks in the Northern Veporic and Northern Gemeric Units (Vozárová et al. 2015, 2016), as well as Central Transdanubia (Szemerédi et al. 2020a) show different REE and other immobile element patterns with negligible negative Eu anomaly and moderate enrichments and depletions (Figs. 8c, 9c). These samples geochemically resemble the porphyric metagranites (Figs. 8e, 9e) in the Eastern Alps (Yuan et al. 2020) drawing a clearly-visibly distinct trend in the La_N vs. La_N/Yb_N diagram (Fig. 8f). According to the zircon U–Pb datings (Fig. 10 and references therein), Late Paleozoic felsic volcanic rocks in the Western Carpathians cover a large timespan from Late Carboniferous (supported by both magmatic and detrital zircon ages; Vozárová et al. 2017, 2018, 2019) to Triassic (Poller et al. 2002; Vozárová et al. 2016) and represent multiple events; however, the obtained ages of the Mid-Permian granite magmatism and A-type felsic volcanism (Vozorává et al. 2012; Ondrejka et al. 2018, 2021; Villaseñor et al. 2021) overlap well with those of the studied rocks (Fig. 10).

Moreover, Mid-Permian radiometric ages, showing similarity to those of the Highiş granitoids, were gained by mafic-intermediate rocks, as well in the Western Carpathians. The latter include zircon and monazite datings of alkali basalt dykes (260.2±1.4 Ma and 259±3 Ma, respectively) in the Tatric Unit (Pelech et al. 2017), zircon U–Pb ages of meta-andesites/metabasalts (263.1±2.6 Ma) in the Veporic Unit (Vozárová et al. 2020), and apatite datings of lamprophyres (263.4±2.6 Ma) in the Malá Fatra Mts. (Spišiak et al. 2018). The correlation of these rocks with the Permian mafic–intermediate lavas in the Codru-Moma Mts. (Fig. 1b) might be the target of future studies; however, in this research we focused on the geochemical and geochronological relationships among the felsic rocks.

Based on the abovementioned findings, correlations are feasible between the Mid-Permian (~270–260 Ma) magmatic rocks in the Tisza Mega-unit and the A-type granitoids in the Central Western Carpathians (267–262 Ma; Ondrejka et al. 2021). Moreover, in the latter area some felsic pyroclastic rocks and lavas showed similar geochemical characteristics and radiometric ages (Gemeric Unit: ~275–269 Ma; Silicic Unit: ~270–263 Ma; Meliata Unit: ~266 Ma; Vozárová et al. 2009, 2012, 2015; Ondrejka et al. 2018) to those of the studied rocks. On the other hand, a group of the felsic (S-type) volcanic rocks in the Western Carpathians (Northern Gemeric and Veporic Units: ~279–272 Ma) and Central Transdanubia (~291–281 Ma) show similar geochemical characteristics to the metagranites in the Eastern Alps (~272–268 Ma).

Such potential correlations, in the aspect of Permian magmatism, among the Europe-derived Tisza Mega-unit and the composite ALCAPA Mega-unit (e.g. Haas et al. 1999; Szederkényi et al. 2013b) further emphasize the complex evolution of the Paleo-Tethyan realm during Late Paleozoic times, where different products were generated in the different areas of the post-orogenic extensional setting. At least two main types of magma source (A and S-types) existed coevally (from the Early Permian to the Earliest Triassic) within this regime in the Central European Variscides (Fig. 10), among which the Highiş granitoids and the associated volcanic rocks in the Tisza Mega-unit (Szemerédi et al. 2020a) unequivocally represent a Mid-Permian (~270–260 Ma) anorogenic, rift-related A-type magmatism.

Conclusions

- Permian granitoid rocks occur in the Highiş massif (SW Apuseni Mts.) with at least three distinct lithologies: (a) medium-grained, equigranular syenogranites, (b) porphyritic microgranites (alkali-feldspar granites), and (c) aplites. All of the studied rocks are peraluminous, subalkaline, alkali-calcic or calc-alkalic, ferroan, and A-type (anorogenic) with granodioritic and subordinate granitic (microgranites, aplites) geochemical compositions and show relatively similar REE and other immobile trace element patterns suggesting their origin from a common or similar source. Trace element compositions refer to the partial melting of the continental crust in the post-collisional extensional setting (continental rifting) of the Paleo-Tethyan realm. Zircon U–Pb datings of medium-grained granites (267.8±4.4, 263.2±4.4, and 262.9±4.1 Ma) revealed a Guadalupian magmatic event, supporting the previous geochronological results (Pană et al. 2002) gained by porphyritic microgranites (264.2±2.3 Ma).
- Based on the very similar trace element compositions and zircon U–Pb ages, the Highiş granitoids have a plutonic–volcanic connection with the Permian felsic volcanic rocks (ignimbrites and subordinate lavas) in the Tisza Mega-unit (Apuseni Mts., basement of the eastern Pannonian Basin, and southern Transdanubia) and represent a Mid-Permian (~270–260 Ma), relatively short-lived (≤10 Myr) magmatic activity. Further connections can be presumed among the other plutonic rocks of the Highiş igneous complex (gabbros, diorites) and the mafic–intermediate lavas (basalts and subordinate andesites) in the Codru-Moma Mts. (western Apuseni Mts.). This potential cogenetic plutonic–volcanic complex in the Tisza Mega-unit could be analogous with the Early Permian bimodal Sesia Magmatic System in the Southern Alps. Plutonic–volcanic connections revealed between the Highiş granitoids and the Permian felsic volcanites in the Tisza Mega-unit suggest that the study area (and

almost certainly the whole Biharia Nappe System) belong to the Tisza Mega-unit as well, despite being assigned to the Dacia Mega-unit in many recent studies.

- Whole-rock geochemistry and zircon U–Pb ages were also applied to gain new information regarding the regional correlations in the area of the Central European Variscides. Despite the Europe-derived nature of the Tisza Mega-unit, the studied magmatism is significantly younger than the similar episodes in stable Europe (300–290 Ma). On the other hand, the Highiş granitoids and the associated volcanic rocks in the Tisza Mega-unit showed correlations with the Late Paleozoic felsic rocks in the ALCAPA Mega-unit (Western Carpathians), including a group of Permian (A-type) volcanic rocks in the Gemeric and Silicic Units and A-type granites (in the Veporic Unit and the Pieniny Klippen Belt). Correlations were also suggested between the Permian (specialized S-type) granites in the Western Carpathians (Gemeric Unit), the porphyric metagranites in the Eastern Alps, and some of the Permian felsic volcanic rocks in the Veporic and Northern Gemeric Units (Western Carpathians), as well as the felsic dykes (Polgárdi) and lavas (Kékkút) in Central Transdanubia that show different geochemical characteristics from the studied rocks of the Tisza Mega-unit.

Acknowledgements: Petrological, geochronological, and correlation studies were financed by the Hungarian National Research, Development and Innovation Office (projects K 131690 and K 108375, project leaders: Elemér Pál-Molnár and Andrea Varga, respectively) and also supported by the New National Excellence Program of the Ministry of Human Capacites (Hungary) to Máté Szemerédi (No. ÚNKP-18-3-I-SZTE-90 supervised by Andrea Varga and ÚNKP-20-4-SZTE-596 supervised by Elemér Pál-Molnár) and Andrea Varga (No. ÚNKP-18-4-SZTE-16). Additionally, this work was financially supported by the Bolyai Research Scholarship of the Hungarian Academy of Sciences (BO/266/18, Andrea Varga). Ioan Seghedi was supported by grant of Ministry of Research and Innovation, CNCS – UEFISCDI, project number PN-III-P4-ID-PCCF-2016-4-0014, within PNCDI III. Field work was additionally supported by Géza Balla and his winery in Păuliş being our kind host during sampling campaigns. We would like to thank Kristóf Fehér (MTA-ELTE Volcanology Research Group) for his assistance in the zircon separation. Furthermore, we are grateful to Martin Ondrejka (Comenius University in Bratislava) and an anonymous reviewer for their suggestions and constructive comments that improved our manuscript.

References

Annen C., Blundy J.D. & Sparks R.S.J. 2006: The Genesis of Intermediate and Silicic Magmas in Deep Crustal Hot Zones. *Journal of Petrology* 47, 505–539. https://doi.org/10.1093/petrology/egi084

Awdankiewicz M. & Kryza R. 2010: The Góry Suche Rhyolitic Tuffs (Intra-Sudetic Basin, SW Poland): preliminary SHRIMP zircon age. *Mineralogia Special Papers* 37, 19.

Bachmann O. & Bergantz G.W. 2004: On the Origin of Crystal-poor Rhyolites: Extracted from Batholithic Crystal Mushes. *Journal of Petrology* 45, 1565–1582. https://doi.org/10.1093/petrology/egh019

Bachmann O. & Bergantz G.W. 2008: Rhyolites and their Source Mushes across Tectonic Settings. *Journal of Petrology* 49, 2277–2285. https://doi.org/10.1093/petrology/egn068

Bachmann O., Miller C.F. & de Silva S.L. 2007: The plutonic–volcanic connection as a stage for understanding crustal magmatism. *Journal of Volcanology and Geothermal Research* 167, 1–23. https://doi.org/10.1016/j.jvolgeores.2007.08.002

Balintoni I. 1997: Geotectonica terenurilor metamorfice din România, Ed. Carpatica, Cluj Napoca. Geotectonics of metamorphic terrains from Romania. *Carpatica Publishouse,* 1–176 (in Romanian).

Balintoni I., Balica C., Cliveti M., Li L.Q., Hann H.P., Chen F. & Schuller V. 2009: The emplacement age of the Muntele Mare Variscan granite (Apuseni Mountains, Romania). *Geologica Carpathica* 60, 495–504. https://doi.org/10.2478/v10096-009-0036-x

Balla Z. 1984: The Carpathian loop and the Pannonian basin: a kinematic analysis. *Geophysical Transactions* 30, 313–353.

Barrat J.-A., Zanda B., Moynier F., Bollinger C., Liorzou C. & Bayon G. 2012: Geochemistry of CI chondrites: Major and trace elements, and Cu and Zn isotopes. *Geochimica et Cosmochimica Acta* 83, 79–92. https://doi.org/10.1016/j.gca.2011.12.011

Bellot N., Boyet M., Doucelance R., Bonnand P., Savov I.P., Plank T. & Eliott T. 2018: Origin of negative cerium anomalies in subduction-related volcanic samples: Constraints from Ce and Nd isotopes. *Chemical Geology* 500, 43–63. https://doi.org/10.1016/j.chemgeo.2018.09.006

Bleahu M. 1976: Structural position of the Apuseni Mts in the Alpine system. *Revue Roumaine de Géologie. Géophysique et Géographie, Série de Géologie* 20, 7–19.

Bleahu M., Lupu M., Patrulius D., Bordea S., Stefan A. & Panin S. 1981: The Structure of the Apuseni Mountains. Guide to Excursion B3. *XII Association Carpatho-Balcanic Congress*, Bucharest, 1–103.

Boehnke P., Watson E.B., Trail D., Harrison T.M. & Schmitt A.K. 2013: Zircon saturation re-revisited. *Chemical Geology* 351, 324–334. https://doi.org/10.1016/j.chemgeo.2013.05.028

Bonin B. 2007: A-type granites and related rocks: Evolution of a concept, problems and prospects. *Lithos* 97, 1–29. https://doi.org/10.1016/j.lithos.2006.12.007

Bonin B. & Tatu M. 2016: Cl-rich hydrous mafic mineral assemblages in the Highiş massif, Apuseni Mountains, Romania. *Mineralogy and Petrology* 110, 447–469. https://doi.org/10.1007/s00710-015-0419-x

Breitkreuz C. & Kennedy A. 1999: Magmatic flare-up at the Carboniferous/Permian boundary in the NE German Basin revealed by SHRIMP zircon ages. *Tectonophysics* 302, 307–326. https://doi.org/10.1016/S0040-1951(98)00293-5

Broska I. & Petrík I. 2015: Variscan thrusting in I- and S-type granitic rocks of the Tribeč Mountains, Western Carpathians (Slovakia): Evidence from mineral compositions and monazite dating. *Geologica Carpathica* 66, 455–471. https://doi.org/10.1515/geoca-2015-0038

Broska I. & Svojtka M. 2020: Early Carboniferous successive I/S granite magmatism recorded in the Malá Fatra Mountains by LA-ICP-MS zircon dating (Western Carpathians). *Geologica Carpathica* 71, 391–401. https://doi.org/10.31577/GeolCarp.71.5.1

Broska I. & Uher P. 2001: Whole-rock Chemistry and Genetic Typology of the West-Carpathian Variscan granites. *Geologica Carpathica* 52, 79–90.

Buda G., Koller F. & Ulrych J. 2004: Petrochemistry of Variscan granitoids of Central Europe: Correlation of Variscan granitoids of the Tisia and Pelsonia Terranes with granitoids of the Moldanubicum, Western Carpathian and Southern Alps. A review: Part I. *Acta Geologica Hungarica* 47, 117–138. https://doi.org/10.1556/ageol.47.2004.2-3.3

Christiansen E.H. 2005: Contrasting processes in silicic magma chambers: Evidence from very large volume ignimbrites. *Geological Magazine* 142, 669–681. https://doi.org/10.1017/S0016756805001445

Christiansen E.H. & McCurry M. 2008: Contrasting origins of Cenozoic silicic rocks from the western Cordillera of the United States. *Bulletin of Volcanology* 70, 251–267. https://doi.org/10.1007/s00445-007-0138-1

Ciobanu C.L., Cook N.J., Damian F. & Damian G. 2006: Gold scavenged by bismuth melts: An example from Alpine shear-remobilizates in the Highiş Mts, Romania. *Mineralogy and Petrology* 87, 351–384. https://doi.org/10.1007/s00710-006-0125-9

Csontos L., Nagymarosy A., Horváth F. & Kovac M. 1992: Tertiary evolution of the intra-Carpathian area: A model. *Tectonophysics* 208, 221–241. https://doi.org/10.1016/0040-1951(92)90346-8

Csontos L. & Vörös A. 2004: Mesozoic plate tectonic reconstruction of the Carpathian region. *Palaeogeography, Palaeoclimatology, Palaeoecology* 210, 1–56. https://doi.org/10.1016/j.palaeo.2004.02.033

Dunkl I., Mikes T., Simon K. & von Eynatten H. 2008: Brief introduction to the Windows program Pepita: data visualization, and reduction, outlier rejection, calculation of trace element ratios and concentrations from LA-ICP-MS data. In: Sylvester P. (Ed.): Laser ablation ICP-MS in the Earth Sciences: Current practices and outstanding issues. *Mineralogical Association of Canada*, 334–340.

Eby G.N. 1992: Chemical subdivision of the A-type granitoids: petrogenetic and tectonic implications. *Geology* 20, 641–644. https://doi.org/10.1130/0091-7613(1992)020<0641:CSOTAT>2.3.CO;2

Frost B.R & Frost C.D. 2008: A geochemical classification for feldspathic igneous rocks. *Journal of Petrology* 49, 1955–1969. https://doi.org/10.1093/petrology/egn054

Frost B.R., Barnes C.G., Collins W.J., Arculus R.J., Ellis D.J. & Frost C.D. 2001: A Geochemical Classification for Granitic Rocks. *Journal of Petrology* 42, 2033–2048. https://doi.org/10.1093/petrology/42.11.2033

Gallhofer D., von Quadt A., Schmid S.M., Guillong M., Peytcheva I. & Seghedi I. 2016: Magmatic and tectonic history of Jurassic ophiolites and associated granitoids from the South Apuseni Mountains (Romania). *Swiss Journal of Geosciences* 110, 699–719. https://doi.org/10.1007/s00015-016-0231-6

Glazner A.F., Coleman D.S. & Bartley J.M. 2008: The tenuous connection between high-silica rhyolites and granodiorite plutons. *Geology* 36, 183–186. https://doi.org/10.1130/G24496A.1

Glazner A.F., Coleman D.S. & Mills R.D. 2015: The volcanic-plutonic connection. In: Breitkreuz C. & Rocchi S. (Eds.): Physical geology of shallow magmatic systems. Advances in volcanology (An Official Book Series of the International Association of Volcanology and Chemistry of the Earth's Interior). *Springer*. https://doi.org/10.1007/978-3-319-14084-1

Haas J., Hámor G. & Korpás L. 1999: Geological setting and tectonic evolution of Hungary. *Geologica Hungarica Series Geologica* 24, 179–196.

Hildreth W. 2004: Volcanological perspectives on Long Valley, Mammoth Mountain, and Mono Craters: Several contiguous but discrete systems. *Journal of Volcanology and Geothermal Research* 136, 169–198. https://doi.org/10.1016/j.jvolgeores.2004.05.019

Horstwood M.S.A., Košler J., Gehrels G., Jackson S.E., McLean N.M., Paton C., Pearson N.J., Sircombe K., Sylvester P., Vermeesch P., Bowring J.F., Condon D.J. & Schoene B. 2016: Community-derived standards for LA-ICP-MS U-(Th)-Pb geochronology – uncertainity propagation, age interpretation and data reporting. *Geostandards and Geoanalytical Research* 40, 311–332. https://doi.org/10.1111/j.1751-908X.2016.00379.x

Hraško Ľ., Broska I. & Finger F. 2002: Permian granitic magmatism and disintegration of the Lower Paleozoic basement in the SW Veporicum near Klenovec (Western Carpathians). In: Michalík J., Šimon L. & Vozár J. (Eds.): *Geologica Carpathica Proceedings of XVII. Congress of Carpathian–Balkan Geological Association*, Bratislava, September 1st–4th, 53, 7.

Ianovici V., Borcoş M., Bleahu M., Patrulius D., Lupu M., Dimitrescu R. & Savu H. 1976: Geology of Apuseni Mts. *Academy Publishouse*, Bucharest, 1–631 (in Romanian).

Ionescu C. & Hoeck V. 2010: Mesozoic ophiolites and granitoids in the Apuseni Mountains. *Acta Mineralogica-Petrographica, Field Guide Series* 20, 44.

Jackson S.E., Pearson N.J., Griffin W.L. & Belousova E.A. 2004: The application of laser ablation-inductively coupled plasma-mass spectrometry to in situ U–Pb zircon geochronology. *Chemical Geology* 211, 47–69. https://doi.org/10.1016/j.chemgeo.2004.06.017

Karakas O., Wotzlaw J.-F., Guillong M., Ulmer P., Brack P., Economos R., Bergantz G.W., Sinigoi S. & Bachmann O. 2019: The pace of crustal-scale magma accretion and differentiation beneath silicic caldera volcanoes. *Geology* 47, 719–723. https://doi.org/10.1130/G46020.1

Kędzior A., Budzyń B., Popa M.E. & Siwecki T. 2020: Monazite U–Th–total Pb age constraints on an early Permian volcanic event in the South Carpathians, Romania. *Geologica Carpathica* 71, 73–82. https://doi.org/10.31577/GeolCarp.71.1.6

Kohút M., Uher P., Putiš M., Ondrejka M., Sergeev S., Larionov A. & Paderin I. 2009: SHRIMP U-Th-Pb zircon dating of the granitoid massifs in the Malé Karpaty Mountain (Western Carpathians): evidence of Meso-Hercynian successive S- to I-type granitic magmatism. *Geologica Carpathica* 60, 345–350. https://doi.org/10.2478/v10096-009-0026-z

Kovács S. 1992: Tethys western ends during the Late Paleozoic and Triassic and their possible genetic relationships. *Acta Geologica Hungarica* 35, 32–369.

Kubiš M. & Broska I. 2010: The granite system near Betliar village (Gemeric Superunit, Western Carpathians): evolution of a composite silicic reservoir. *Journal of Geosciences* 55, 131–148. https://doi.org/10.3190/jgeosci.066

Le Maitre R.W., Streckeisen A., Zanettin B., Le Bas M.J., Bonin B. & Bateman P. 1989: Igneous rocks: A classification and glossary of terms. Recommendations of the International Union of Geological Sciences Subcomission on the Systematics of Igneous Rocks. *Blackwell*, Oxford, 1–256.

Lelkes-Felvári Gy. & Klötzli U. 2004: Zircon geochronology of the „Kékkút quartz porphyry", Balaton Highland, Transdanubian Central Range, Hungary. *Acta Geologica Hungarica*, 47, 139–149. https://doi.org/10.1556/ageol.47.2004.2-3.4

Ludwig K.R. 2012: User's manual for Isoplot 3.75: A geochronological Toolkit for Microsoft Excel. *Berkeley Geochronology Center Special Publication* No. 4.

Lützner H., Tichomirowa M., Käßner A. & Gaupp R. 2021: Latest Carboniferous to early Permian volcano-stratigraphic evolution in Central Europe: U–Pb CA–ID–TIMS ages of volcanic rocks in the Thuringian Forest Basin (Germany). *International Journal of Earth Sciences* 110, 377–398. https://doi.org/10.1007/s00531-020-01957-y

McLennan S.M. 1989: Rare Earth Elements in Sedimentary Rocks: Influence of Provenance and Sedimentary Processes. In: Lipin B.R. et al. (Eds.): Geochemistry and Mineralogy of Rare Earth Elements. *Reviews in Mineralogy* 21, 169–200.

Nicolae I., Seghedi I., Boboş I., Azevedo M.R., Ribeiro S. & Tatu M. 2014: Permian volcanic rocks from the Apuseni Mountains (Romania): Geochemistry and tectonic constrains. *Chemie der Erde* 74, 125–137. https://doi.org/10.1016/j.chemer.2013.03.002

Ondrejka M., Li X.H., Vojtko R., Putiš M., Uher P. & Sobocký T. 2018: Permian A-type rhyolites of the Muraň Nappe, Inner Western Carpathians, Slovakia: in-situ zircon U–Pb SIMS ages and tectonic setting. *Geologica Carpathica* 69, 187–198. https://doi.org/10.1515/geoca-2018-0011

Ondrejka M., Uher P., Putiš M., Kohút M., Broska I., Larionov A., Bojar A.-V. & Sobocký T. 2021: Permian A-type granites of the Western Carpathians and Transdanubian regions: products of the Pangea supercontinent breakup. *International Journal of Earth Sciences* 110, 2133–2155. https://doi.org/10.1007/s00531-021-02064-2

Petrík I. & Kohút M. 1997: The evolution of granitoid magmatism during the Hercynian orogen in the Western Carpathians. *Mineralia Slovaca - Monograph* 235–252.

Pál-Molnár E., András E., Kassay Z., Buda G. & Batki A. 2008: Petrology of Păuliş Granites (Apuseni Mts., Romania). *Acta Mineralogica–Petrographica* 48, 33–41.

Pană D.I. & Balintoni I. 2000: Igneous protoliths of the Biharia lithotectonic assemblage: timing of intrusion, geochemical considerations, tectonic setting. *Studia Universitatis Babeş-Bolyai* 45, 1. https://doi.org/10.5038/1937-8602.45.1.1

Pană D.I., Heaman L.M., Creaser R.A. & Erdmer, P. 2002: Pre-alpine crust in the Apuseni Mountains, Romania: insights from Sm–Nd and U–Pb data. *The Journal of Geology* 110, 341–354. https://doi.org/10.1086/339536

Pearce J.A., Harris N.B.W. & Tindle A.G. 1984: Trace element discrimination diagrams for the tectonic interpretation of granitic rocks. *Journal of Petrology* 24, 956–983. https://doi.org/10.1093/petrology/25.4.956

Pelech O., Vozárová A., Uher P., Petrík I., Plašienka D., Šarinová K. & Rodionov N. 2017: Late Permian volcanic dykes in the crystalline basement of the Považský Inovec Mts. (Western Carpathians): U–Th–Pb zircon SHRIMP and monazite chemical dating. *Geologica Carpathica* 68, 530–542. https://doi.org/10.1515/geoca-2017-0035

Poller U., Uher P., Broska I., Plasienka D. & Janák M. 2002: First Permian±Early Triassic zircon ages for tin-bearing granite from the Gemeric unit (Western Carpathians, Slovakia): connection to the post-collisional extension of the Variscan orogen and S-type granite magmatism. *Terra Nova* 14, 41–48. https://doi.org/10.1046/j.1365-3121.2002.00385.x

Putiš M., Kotov A.B., Uher P., Salnikova E.B. & Korikovsky S.P. 2000: Triassic age of the Hroncok pre-orogenic A-type granite related to continental rifting: A new result of U-Pb isotope dating (Western Carpathians). *Geologica Carpathica* 51, 59–66.

Radvanec M., Konečný P., Ondrejka M., Putiš M., Uher P. & Németh Z. 2009: The Gemeric granites as an indicator of the crustal extension above the Late-Variscan subduction zone and during the Early Alpine riftogenesis (Western Carpathians): An interpretation from the monazite and zircon ages dated by CHIME and SHRIMP methods. *Mineralia Slovaca* 41, 381–394 (in Slovak with English abstract).

Repstock A., Breitkreuz C., Lapp M. & Schulz B. 2017: Voluminous and crystal-rich igneous rocks of the Permian Wurzen volcanic system, northern Saxony, Germany: physical volcanology and geochemical characterization. *International Journal of Earth Sciences* 107, 1485–1513. https://doi.org/10.1007/s00531-017-1554-x

Roduit N. 2019: JMicroVision: Image analysis toolbox for measuring and quantifying components of high-definition images. Version 1.3.1. https://jmicrovision.github.io

Rojkovič I. & Konečný P. 2005: Th–U–Pb dating of monazite from the Cretaceous uranium vein mineralization in the Permian rocks of the Western Carpathians. *Geologica Carpathica* 56, 493–502.

Rudnick R.L. & Gao S. 2003: Composition of the Continental Crust. *Treatise on geochemistry* 3, 1–64. https://doi.org/10.1016/B0-08-043751-6/03016-4

Săndulescu M. 1984: Geotectonics of Romania. *Technical Publishouse*, Bucharest, 1–336 (in Romanian).

Schmid S.M., Bernoulli D., Fügenschuh B., Matenco L., Schefer S., Schuster R., Tischler M. & Ustaszewski K. 2008: The Alpine–Carpathian–Dinaridic orogenic system: correlation and evolution of tectonic units. *Swiss Journal of Geosciences* 101, 139–183. https://doi.org/10.1007/s00015-008-1247-3

Schmid S.M., Fügenschuh B., Kounov A., Matenco L., Nievergelt P., Oberhänsli R., Pleuger J., Schefer S., Schuster R., Tomljenović B., Ustaszewski K. & van Hinsbergend D.J.J. 2020: Tectonic units of the Alpine collision zone between Eastern Alps and western Turkey. *Gondwana Research* 78, 308–374. https://doi.org/10.1016/j.gr.2019.07.005

Shand S.J. 1943: Eruptive rocks. Their genesis composition, classification, and their relation to ore-deposits with a chapter on meteorite. *John Wiley & Sons*, New York, 1–488.

Sinigoi S., Quick J.E., Demarchi G. & Peressini G. 2010: The Sesia Magmatic System. *Journal of the Virtual Explorer* 36, 4. https://doi.org/10.3809/jvirtex.2010.00218

Sláma J., Košler J., Condon D.J., Crowley J.L., Gerdes A., Hanchar J.M., Horstwood M.S.A., Morris G.A., Nasdala L., Norberg N., Schaltegger U., Schoene B., Tubrett M.N. & Whitehouse M.J. 2008: Plešovice zircon – A new natural reference material for U–Pb dating and Hf isotopic microanalyses. *Chemical Geology* 249, 1–35. https://doi.org/10.1016/j.chemgeo.2007.11.005

Słodczyk E., Pietranik A., Glynn S., Wiedenbeck M., Breitkreuz C. & Dhuime B. 2018: Contrasting sources of Late Paleozoic rhyolite magma in the Polish Lowlands: evidence from U–Pb age and Hf and O isotope composition in zircon. *International Journal of Earth Sciences* 107, 2065. https://doi.org/10.1007/s00531-018-1588-8

Spišiak J., Vetráková L., Chew D., Ferenc Š., Mikuš T., Šimonová V. & Bačík P. 2018: Petrology and dating of the Permian lamprophyres from the Malá Fatra Mts. (Western Carpathians, Slovakia). *Geologica Carpathica* 69, 453–466. https://doi.org/10.1515/geoca-2018-0026

Stampfli G.M. & Kozur H.W. 2006: Europe from the Variscan to the Alpine cycles. In: Gee D.G. & Stephenson R.A. (Eds.): European Lithosphere Dynamics. *Geological Society, London,Memoirs*, 32, 57–82. https://doi.org/10.1144/GSL.MEM.2006.032.01.04

Sun S.S. & McDonough W.F. 1989: Chemical and isotopic systematic of oceanic basalts implications for mantle compositions and processes. In: Saunders A.D. & Norry M.J. (Eds): Magmatism in ocean basins. *Geological Society London Special Publication* 42, 312–345.

Szederkényi T., Haas J., Nagymarosy A. & Hámor G. 2013a: Geology and History of Evolution of the Tisza Mega-unit. In: Haas J. (Ed.): Geology of Hungary. *Regional Geology Reviews*, *Springer*, 103–148. https://doi.org/10.1007/978-3-642-21910-8

Szederkényi T., Kovács S., Haas J. & Nagymarosy A. 2013b: Geology and history of evolution of the ALCAPA Mega-Unit. In: Haas J. (Ed.): Geology of Hungary. *Regional Geology Reviews*, *Springer*, 1–102. https://doi.org/10.1007/978-3-642-21910-8

Szemerédi M., Varga A., Lukács R. & Pál-Molnár E. 2016: Petrography of the Gyűrűfű Rhyolite Formation, Western Mecsek Mts, Hungary. *Földtani Közlöny* 146, 335–354 (in Hungarian with English abstract).

Szemerédi M., Varga A., Lukács R. & Pál-Molnár E. 2017: Petrography of the Gyűrűfű Rhyolite Formation, northern foreland of the Villány Mts, Hungary. *Földtani Közlöny* 147, 357–382. (in

Hungarian with English abstract). https://doi.org/10.23928/foldt.kozl.2017.147.4.357

Szemerédi M., Lukács R., Varga A., Dunkl I., Józsa S., Tatu M., Pál-Molnár E., Szepesi J. Guillong M., Szakmány G. & Harangi S. 2020a: Permian felsic volcanic rocks in the Pannonian Basin (Hungary): new petrographic, geochemical and geochronological results. *International Journal of Earth Sciences* 109, 101–125. https://doi.org/10.1007/s00531-019-01791-x

Szemerédi M., Varga A., Szepesi J., Pál-Molnár E. & Lukács R. 2020b: Lavas or ignimbrites? Permian felsic volcanic rocks of the Tisza Mega-unit (SE Hungary) revisited: A petrographic study. *Central European Geology* 63, 1–18. https://doi.org/10.1556/24.2020.00003

Tavazzani L., Peres S., Sinigoi S., Demarchi G., Economos R.C. & Quick J.E. 2020: Timescales and Mechanisms of Crystal-mush Rejuvenation and Melt Extraction Recorded in Permian Plutonic and Volcanic Rocks of the Sesia Magmatic System (Southern Alps, Italy). *Journal of Petrology* 61, 5. https://doi.org/10.1093/petrology/egaa049

Tischler M., Matenco L., Filipescu S., Gröger H.R., Wetzel A. & Fügenschuh B. 2008: Tectonics and sedimentation during convergence of the ALCAPA and Tisza–Dacia continental blocks: the Pienide nappe emplacement and its foredeep (N. Romania). *Geological Society London Special Publications* 298, 317–334. https://doi.org/10.1144/SP298.15

Uher P. & Broska I. 1996: Post-orogenic Permian granitic rocks in the Western Carpathian-Pannonian area: geochemistry, mineralogy and evolution. *Geologica Carpathica* 47, 311–321.

Uher P. & Ondrejka M. 2009: The Velence granites, Transdanubic Superunit: a product of Permian A-type magmatism and Alpine overprint (results of zircon SHRIMP and monazite EMPA dating). Proceedings of the 7th Meeting of the Central European Tectonic Studies Group (CETeG) and 14th Meeting of the Czech Tectonic Studies Group (CTS), *HUNTEK-2009*, Pécs, Abstracts, 32.

Varga A. & Raucsik B. 2014: Pedogenic calcrete records in southern Transdanubia, Hungary: A brief review with paleoenvironmental and paleogeographic implications. *Central European Geology* 57, 137–151. https://doi.org/10.1556/ceugeol.57.2014.2.2

Vermeesch P. 2018: IsoplotR: a free and open toolbox for geochronology. *Geoscience Frontiers* 9, 1479–1493. https://doi.org/10.1016/j.gsf.2018.04.001

Villaseñor G., Catlos E.J., Broska I., Kohút M., Hraško Ľ, Aguilera K., Etzel T.M., Kyle J.R. & Stockli D.F. 2021: Evidence for widespread mid-Permian magmatic activity related to rifting following the Variscan orogeny (Western Carpathians). *Lithos* 390–391, 106083. https://doi.org/10.1016/j.lithos.2021.106083

Vozárová A., Šmelko M. & Paderin I. 2009: Permian single crystal U–Pb age of the Rožňava Formation volcanites (Southern Gemeric Unit, Western Carpathians, Slovakia). *Geologica Carpathica* 60, 439–448. https://doi.org/10.2478/v10096-009-0032-1

Vozárová A., Šmelko M., Paderin I. & Larionov A. 2012: Permian volcanics in the Northern Gemericum and Bôrka Nappe system: U–Pb zircon dating and the implications for geodynamic evolution (Western Carpathians, Slovakia). *Geologica Carpathica* 63, 191–200. https://doi.org/10.2478/v10096-012-0016-4

Vozárová A., Presnyakov S., Šarinová K. & Šmelko M. 2015: First evidence for Permian–Triassic boundary volcanism in the Northern Gemericum: geochemistry and U–Pb zircon geochronology. *Geologica Carpathica* 66, 375–391. https://doi.org/10.1515/geoca-2015-0032

Vozárová A., Rodionov N., Vozár J., Lepekhina E. & Šarinová K. 2016: U–Pb zircon ages from Permian volcanic rocks and tonalite of the Northern Veporicum (Western Carpathians). *Journal of Geosciences* 61, 221–237. https://doi.org/10.3190/jgeosci.215

Vozárová A., Larionov A., Šarinová K., Vďačný M., Lepekhina E., Vozár J. & Lvov P. 2017: Detrital zircons from the Hronicum Carboniferous–Permian sandstones (Western Carpathians, Slovakia): depositional age and provenance. *International Journal of Earth Sciences* 107, 1539–1555. https://doi.org/10.1007/s00531-017-1556-8

Vozárová A., Larionov A., Šarinová K., Rodionov N., Lepekhina E., Vozár J. & Paderin I. 2018: Clastic wedge provenance in the Zemplinicum Carboniferous–Permian rocks using the U–Pb zircon age dating (Western Carpathians, Slovakia). *International Journal of Earth Sciences* 108, 115–135. https://doi.org/10.1007/s00531-018-1645-3

Vozárová A., Šarinová K., Laurinc D., Lepekhina E., Vozár J., Rodionov N. & Lvov P. 2019: Exhumation history of the Variscan suture: Constrains on the detrital zircon geochronology from Carboniferous–Permian sandstones (Northern Gemericum; Western Carpathians). *Geologica Carpathica* 70, 512–530. https://doi.org/10.2478/geoca-2019-0030

Vozárová A., Šarinová K., Rodionov N. & Vozár J. 2020: Zircon U–Pb geochronology from Permian rocks of the Tribeč Mts. (Western Carpathians, Slovakia). *Geologica Carpathica* 71, 274–287. https://doi.org/10.31577/GeolCarp.71.3.6

Whalen J.B., Currie K.L. & Chapell B.W. 1987: A-type granites: geochemical characteristics, discrimination and petrogenesis. *Contributions to Mineralogy and Petrology* 95, 407–419. https://doi.org/10.1007/BF00402202

Wiedenbeck M., Allé P., Corfu F., Griffin W.L., Meier M., Oberli F., von Quadt A., Roddick J.C. & Spiegel W 1995: Three natural zircon standards for U–Th–Pb, Lu–Hf trace element and REE analyses. *Geostandards Newsletter* 19, 1–23. https://doi.org/10.1111/j.1751-908x.1995.tb00147.x

Winchester J.A. & Floyd P.A. 1977: Geochemical discrimination of different magma series and their differentiation products using immobilile elements. *Chemical Geology* 20, 325–343. https://doi.org/10.1016/0009-2541(77)90057-2

Yuan S., Neubauer F., Liu Y., Genser J., Lui B., Yu S., Chang R. & Guan Q. 2020: Widespread Permian granite magmatism in Lower Austroalpine units: significance for Permian rifting in the Eastern Alps. *Swiss Journal of Geosciences* 113, 18. https://doi.org/10.1186/s00015-020-00371-5

Electronic supplementary material is available online:

Supplementary Table S1 at http://geologicacarpathica.com/data/files/supplements/GC-72-6-Szemeredi_Table_S1.xls
Supplementary Fig. S1 at http://geologicacarpathica.com/data/files/supplements/GC-72-6-Szemeredi_Fig_S1.pdf